The Journal of Neuroscience, May 1993, 13(5): 2085–2104

Source Specificity of Early Calcium Neurotoxicity in Cultured Embryonic Spinal Neurons

Michael Tymianski,[1] Milton P. Charlton,[1,2] Peter L. Carlen,[1] and Charles H. Tator[1]

[1]Playfair Neuroscience Unit, University of Toronto, Toronto, Ontario M5T 2S8, and [2]Physiology Department MSB, University of Toronto, Toronto, Ontario M5S 1A8, Canada

To examine the role of Ca^{2+} in early neuronal death, we studied the impact of free intracellular calcium concentration ($[Ca^{2+}]_i$) on survivability in populations of cultured mouse spinal neurons. We asked whether early neurotoxicity was triggered by Ca^{2+} influx, whether elevated $[Ca^{2+}]_i$ was a predictive indicator of impending neuronal death, and whether factors other than $[Ca^{2+}]_i$ increases influenced Ca^{2+} neurotoxicity. We found that when neurons were lethally challenged with excitatory amino acids or high K^+, they experienced a biphasic $[Ca^{2+}]_i$ increase characterized by a primary $[Ca^{2+}]_i$ transient that decayed within minutes, followed by a secondary, sustained, and irreversible $[Ca^{2+}]_i$ rise that indicated imminent cell death. We showed that in the case of glutamate-triggered neurotoxicity, processes triggering eventual cell death required Ca^{2+} influx, and that neurotoxicity was a function of the transmembrane Ca^{2+} gradient. Fura-2 Ca^{2+} imaging revealed a "ceiling" on measurable changes in $[Ca^{2+}]_i$ that contributed to the difficulty in relating $[Ca^{2+}]_i$ to neurotoxicity. We found, by evoking Ca^{2+} influx into neurons through different pathways, that the chief determinants of Ca^{2+} neurotoxicity were the Ca^{2+} source and the duration of the Ca^{2+} challenge. When Ca^{2+} source and challenge duration were taken into account, a statistically significant relationship between measured $[Ca^{2+}]_i$ and cell death was uncovered, although the likelihood of neuronal death depended much more on Ca^{2+} source than on the magnitude of the measured $[Ca^{2+}]_i$ increase. Thus, neurotoxicity evoked by glutamate far exceeded that evoked by membrane depolarization with high K^+ when $[Ca^{2+}]_i$ was made to increase equally in both groups. The neurotoxicity of glutamate was triggered primarily by Ca^{2+} influx through NMDA receptor channels, and exceeded that triggered by non-NMDA receptors and Ca^{2+} channels when $[Ca^{2+}]_i$ was made to rise equally through these separate pathways. The greater neurotoxicity triggered by NMDA receptors was related to some attribute other than an ability to trigger greater $[Ca^{2+}]_i$ increases as compared with other Ca^{2+} sources. We hypothesize that this represents a physical colocalization of NMDA receptors with Ca^{2+}-dependent rate-limiting processes that trigger early neuronal degeneration.

[Key words: calcium, spinal neurons, glutamate receptors, NMDA receptors, neurotoxicity, fura-2]

Calcium influx into cells has been termed the "final common pathway of cell death" (Schanne et al., 1979). Since then, an excessive or sustained intracellular Ca^{2+} accumulation has been implicated as a trigger for neuronal degeneration (for reviews, see Choi, 1988; Meyer, 1989; Siesjo and Bengtsson, 1989; Farooqui and Horrocks, 1991). The Ca^{2+} neurotoxicity hypothesis is consistent with the observation that Ca^{2+} accumulates in nervous tissue in cerebral ischemia (Siesjo, 1988; Siesjo and Bengtsson, 1989; Uematsu et al., 1991), in epilepsy (Meyer, 1989; Uematsu et al., 1990), and possibly in trauma (Balentine, 1988; Faden et al., 1989). In these disorders, neuronal Ca^{2+} overload may be triggered by several mechanisms, the most noted of which is the toxic release of the excitatory neurotransmitter glutamate through synaptic overactivity (for review, see Rothman and Olney, 1987). Considerable experimental evidence supports the notion that excessive exposure to certain excitatory amino acids (EAAs) causes Ca^{2+} influx and neurotoxicity (Rothman, 1984; Choi, 1985, 1987; Rothman and Olney, 1986; Choi et al., 1987; Murphy et al., 1988; Scharfman and Schwartzkroin, 1989; Randall and Thayer, 1992). Ca^{2+} influx has been associated with early neuronal degeneration arising within minutes following a brief EAA challenge (Randall and Thayer, 1992), or with delayed neurotoxicity occurring up to many hours following the initial insult (Choi et al., 1987; Rothman et al., 1987; Koh and Choi, 1991; Weiss et al., 1990). However, although many studies implicate Ca^{2+} influx in the neurotoxic process (Jancso et al., 1984; Choi, 1985; Garthwaite et al., 1986; W. J. Goldberg et al., 1986; Olney et al., 1986; Choi, 1987; Murphy et al., 1988; Ellren and Lehmann, 1989; M. P. Goldberg et al., 1989; Kurth et al., 1989; Marcoux et al., 1990), its contribution to toxicity following an insult has been difficult to separate from that of a multitude of non-Ca^{2+}-dependent processes set in motion at the same time (e.g., activation of Na^+, K^+, and Cl^- conductances; see Rothman, 1985). A further problem in establishing a clear link between Ca^{2+} influx and toxicity has been the difficulty in demonstrating a relationship between Ca^{2+} load and neuronal death: while some reports suggest a correlation between the magnitude of the rise in free intracellular calcium concentration ($[Ca^{2+}]_i$) and neurotoxicity (Milani et al., 1991), others could not demonstrate such associations (Michaels and Rothman, 1990; Dubinsky and Rothman, 1991). Moreover, some studies provide evidence that is

Received July 20, 1992; revised Oct. 20, 1992; accepted Nov. 18, 1992.

This work was supported by a grant from the Network on Neural Recovery and Regeneration of the Networks of Centres of Excellence of Canada, and a grant from the Samuel Lunenfeldt Foundation. M.T. is a research fellow of the Medical Research Council of Canada.

Correspondence should be addressed to Dr. Michael Tymianski, Lab 12-423, MC-PAV, Playfair Neuroscience Unit, Toronto Western Division, Toronto Hospital, 399 Bathurst Street, Toronto, Ontario, M5T 2S8, Canada.

seemingly contradictory to the Ca^{2+} hypothesis (e.g., Price et al., 1985; Lemasters et al., 1987; Collins et al., 1991). Given this controversy, a causal link between Ca^{2+} influx and neuronal death needs further investigation.

The present experiments, therefore, were designed to clarify the role of Ca^{2+} as a trigger for neurotoxicity in an attempt to reconcile the difficulties and controversies outlined above. To this end, we developed a assay in which large numbers of individual neurons were studied quantitatively with respect to their $[Ca^{2+}]_i$ dynamics, Ca^{2+} influx pathways, and the temporal relationships between neuronal Ca^{2+} loading and death. This report addresses the following questions. Is there a measurable relationship between Ca^{2+} influx and neurotoxicity? Is a large rise in neuronal $[Ca^{2+}]_i$ a sufficient trigger for neurotoxicity? Is one Ca^{2+} influx pathway more neurotoxic than others? Is the degree of neurotoxicity evoked by activating a given Ca^{2+} influx pathway (e.g., the NMDA receptor channel) solely a function of that pathway's ability to generate a large Ca^{2+} flux?

Materials and Methods

Tissue culture. Spinal neurons from E13 fetal Swiss mice were cultured for 2 weeks on glass coverslips coated with poly-D-lysine hydrobromide (MW, 30,000–70,000; Sigma, P-7280). Dorsal root ganglia were excluded during the dissection. For some experiments, the neurons were grown in explants of cervical or lumbar spinal cord as described by Gahwiler (1981), and in others they were grown as conventional dissociated primary neuronal cultures (Guthrie et al., 1987). There were no noticeable differences in neuronal density or morphology between explants cultured from cervical and lumbar spinal segments. All cultures were maintained in a humidified 5% CO_2, 95% air atmosphere at 36.5°C, and were fed biweekly with a medium containing 58% minimum essential medium (MEM; GIBCO 410-1100), 20% fetal bovine serum, and 20% distilled water, supplemented with (in mM) 40 glucose, 11.6 $NaHCO_3$, 0.4 L-glutamine and insulin, 80 biological units/100 ml of medium, balanced to 300 mOsm and pH 7.4 in 5% CO_2. At 4 d *in vitro*, the dissociated cultures were treated with 20μg/ml 5′-fluorodeoxyuridine and 50 μg/ml uridine for 24 hr to inhibit proliferation of non-neuronal cells. Antimitotics were not used for explant cultures, and no antibiotics were employed. The presence of neurons and astrocytes in the cultures was confirmed by immunocytochemical staining for neurofilament, neuron-specific enolase, and glial fibrillary-associated protein (E. Theriault and M. Tymianski, unpublished observations).

Loading of neurons with calcium indicator. The cultures were incubated for 60 min in loading medium (78% MEM and 20% distilled water, supplemented to 40 mM D-glucose, 1.0 mM Mg^{2+}, and 20 mM HEPES, pH 7.4, in 5% CO_2) containing 1 μM fura-2 acetoxymethyl ester (fura-2/AM; Molecular Probes Inc.) in a final concentration of 0.2% dimethyl sulfoxide (DMSO). The lipophilic membrane-permeant fura-2/AM penetrates into neurons, and is converted by the action of intracellular esterases into the membrane-impermeant fura-2 salt, which is trapped intracellularly as a specific calcium indicator (Grynkiewicz et al., 1985). After loading, the cultures were washed for 30 min in loading medium without fura-2 to attenuate any background fluorescence from residual extracellular indicator. The fura-2 fluorescence from individual neurons was readily visualized in both dissociated and explant cultures despite the thickness of the latter (50–75 μm). Neurons fluoresced more intensely than glia and other large cells (Connor et al., 1987).

Instrumentation. Cultures loaded with indicator were mounted in a microscope-stage incubator (Medical Systems Corp. model TC-202), and viewed with an inverted microscope (Nikon Diaphot-TMD equipped with xenon epifluorescence optics) through a fluorite oil-immersion lens (Nikon CF UV-F; 40×, 1.3 NA) in contact with the coverslip bottom. A second-generation microchannel-plate intensified CCD-array camera (Quantex Corp. model QX-100) recorded the 510 nm fluorescence emissions from fura-2 in neurons excited through narrow band-pass filters (340 ± 5 nm, 380 ± 6.5 nm; Omega Optical) housed in a computer-controlled filter wheel. All data were gathered on a 80386-based computer, and were archived on an optical disk drive (Panasonic, LF-5010). The system allowed for a maximal time resolution of 2 sec between successive $[Ca^{2+}]_i$ measurements.

Calibration. $[Ca^{2+}]_i$ was determined using *in vitro*–derived conversion factors used to generate a calibration curve described by the equation $[Ca^{2+}]_i = K_d(F_{min}/F_{max})[(R - R_{min})/(R_{max} - R)]$, in which K_d = 224 nM, the dissociation constant for fura-2 (Grynkiewicz et al., 1985; for reviews, see Goldman et al., 1990; Moore et al., 1990). To determine (F_{min}/F_{max}), R_{min}, and R_{max}, we imaged a glass-bottom slide with 100 μl chambers containing control solution (see below), 1 μM fura-2 pentapotassium salt, and either a saturating calcium load (1 mM) or zero calcium with 10 mM EGTA. A third chamber containing control solution without fura-2 was used to generate background images. Typical values for conversion factors were F_{min}/F_{max} = 10.31, R_{min} = 0.54, and R_{max} = 10.48. During experiments, ratio images were generated by gathering and averaging eight raw fluorescence images from neurons at each wavelength (340 nm and 380 nm). Each average was corrected for background fluorescence and camera dark current by subtracting a frame gathered at the beginning of each experiment at each excitation wavelength from an area of the coverslip devoid of cells (Connor et al., 1987). The images were then converted on line to calibrated fura-2 ratio images (340 nm/380 nm) using a pseudocolor display of $[Ca^{2+}]_i$. $[Ca^{2+}]_i$ for individual neurons was determined by averaging the $[Ca^{2+}]_i$ values for all the pixels within a boundary traced around the perimeter of the cell soma prior to starting the experiment. The system was recalibrated following any adjustments to the apparatus. We were unable to reproduce in our neuronal preparation the *in vivo* calibrations described by others for non-neuronal cells (e.g., Williams and Fay, 1990), because when spinal neurons were exposed to varying concentrations of calcium ionophore (4-bromo-A23187, 0.5–10 μM), the increase in the fura-2 fluorescence was always interrupted by cell lysis prior to reaching a stable end-point. In pilot experiments, the highest value of R_{max} obtained immediately prior to lysis was variable (in the 5–7 range), but exceeded the highest ratio values observed when $[Ca^{2+}]_i$ transients were elicited in neurons in the present experiments (see below). Our methods precluded the determination of R_{max} by applying Ca^{2+} ionophore at the end of each experiment, because cell membrane integrity was a critical outcome measure in the present investigations.

Drugs and solutions. The control solution contained (in mM) 130 NaCl, 1.3 $CaCl_2$, 4.5 KCl, 22 D-glucose, 20 HEPES, 1.0 sodium pyruvate, and 0.001 glycine. Glycine was omitted in experiments where activation of NMDA receptors was undesirable. To produce the 50 mM K^+ solution, 45.5 mM of KCl were substituted for NaCl. To produce the low-Na solution, NaCl (130 mM) was omitted and replaced by 130 mM choline-Cl. All solutions were adjusted to 300 mOsm, pH 7.4, and 36.5°C prior to administration. Nimodipine (Miles Pharmaceuticals Inc.) and 6-cyano-7-nitroquinoxaline (CNQX; Research Biochemicals Inc.) stock solutions were prepared in DMSO. ω-Conotoxin GVIA (3 mM; Bachem Inc.) stock was prepared in distilled water. These were stored at −20°C. All other agents were prepared daily in control solution. During experiments, the final DMSO concentrations never exceeded 0.2%, a level that had no effect on $[Ca^{2+}]_i$ or on neuronal survival in pilot studies.

Neuronal viability assays. Following each experiment, the cultures were incubated for 10 min at 36.5°C with 2μM ethidium homodimer and 1μM calcein/AM. Ethidium homodimer binds to nuclear material in dead cells, whereas calcein/AM, by virtue of the enzymatic hydrolysis of the ester, is retained in living cells (Moore et al., 1990). Thus, when excited in the fluorescein range (485–500 nm), dead cells appear red-orange, whereas living cells appear green (Fig. 1*C*). As a further measure of cell viability, the cultures were also superfused for 2 min with 0.4% trypan blue stain (Fig. 1*B*), and neuronal viability was confirmed with bright-field microscopy.

Experimental procedure. All experiments were performed at 36.5 ± 5°C. Neurons loaded with fura-2 were superfused with control solution at 1–2 ml/min. $[Ca^{2+}]_i$ was measured simultaneously in several neurons in the field throughout the experiments. Baseline $[Ca^{2+}]_i$ was registered for 5–15 min, following which the neurons were exposed to a 50 min challenge with either 250 μM glutamate, 50 mM K^+ (high K^+), 100 μM NMDA, or 100 μM kainate. The rise in neuronal $[Ca^{2+}]_i$ was measured about every 2 sec from the onset of the challenge until peak $[Ca^{2+}]_i$ was registered. Then, the frequency of $[Ca^{2+}]_i$ measurements was gradually reduced as $[Ca^{2+}]_i$ declined, reaching a measurement every 3 min when the decay in $[Ca^{2+}]_i$ ended. Following the 50 min challenge, neurons in some experiments were again superfused with control solution for a further 30 min. The 2 sec interval between successive $[Ca^{2+}]_i$ measurements sufficed to resolve the time course of most $[Ca^{2+}]_i$ transients, because the average half-time to peak at 36.5°C was 16.8 ± 2.4 sec

Table 1. Relationship between Ca^{2+} deregulation and vital staining of dead neurons

	Total deregulated	Total stained	% stained	No. of experiments
Trypan blue	634	628	99.05	107
Ethidium homodimer	296	148	50.00	34

The neurons were incubated with the vital stains following a 50 min challenge with EAAs (NMDA, kainate, or glutamate) as described in Materials and Methods. The number of neurons undergoing Ca^{2+} deregulation and vital staining was counted in each experiment. Total deregulated, total number of neurons that underwent Ca^{2+} deregulation; total stained, total number of neurons staining with the indicator.

(mean ± SEM; see Fig. 7*D*, inset), and the typical peaks lasted between 6 and 20 sec, depending on the stimulus duration (see Figs. 5*B*, 7*D*, insets).

Data analysis and display. Statistical analyses were performed using ANOVA with post hoc multiple comparisons using the Newman–Keuls procedure to determine significant differences between individual group means (see section 7.4 in Armitage and Berry, 1987). Linear and logistic regression analyses were employed to model and test probabilities of cell death. Where appropriate, survival analysis methods using the Kaplan–Meier survival model (see section 14.5 in Armitage and Berry, 1987) were employed to test time-dependent effects. Unless otherwise stated, mean values are provided with their standard errors (mean ± SE). When plotting the time course of neuronal $[Ca^{2+}]_i$ (e.g., Fig. 1*A*), if the measured $[Ca^{2+}]_i$ eventually rose to values exceeding those of the meaningful range of the calibration curve, the tracings were truncated for the purpose of clarity at values around 1500 nM $[Ca^{2+}]_i$ (asterisks).

Calculation of $[Ca^{2+}]_i$ parameters. These are defined as in Figure 3*A*. The parameters were calculated individually for each neuron challenged with a Ca^{2+} load. In the experiments shown in Figures 3, 4, 7, and 10, peak $[Ca^{2+}]_i$ was taken as the highest value of $[Ca^{2+}]_i$ registered during the initial $[Ca^{2+}]_i$ transient. The calcium–time index (CTI; see Fig. 7), a measure of the total Ca^{2+} load evoked by a given challenge (high K^+ or EAAs) was calculated by integrating $[Ca^{2+}]_i$ over time from the Ca^{2+} challenge onset, up to—but excluding—the time of Ca^{2+} deregulation or the experimental end-point (whichever came first). Average $[Ca^{2+}]_i$, the mean value of $[Ca^{2+}]_i$ throughout a challenge (see Figs. 3, 4, 7, 10), was taken as the CTI (area under the curve) divided by the time interval over which CTI was computed (i.e., the average value of a function). The criteria by which the time of onset of $[Ca^{2+}]_i$ deregulation was determined are shown in Figure 3*A*.

Results

The digital imaging approach permitted the simultaneous measurement of $[Ca^{2+}]_i$ in several cells per experiment (range, 4–27), for a total of over a thousand neurons in the studies outlined below. Of these, 39 neurons (approximately 4%) were excluded from analysis because of persistently elevated $[Ca^{2+}]_i$ (>250 nM) during baseline measurements. All neurons were cultured for 14–17 d to obtain a high susceptibility to glutamate neurotoxicity that was uniform between cultures (Regan and Choi, 1991). At this stage *in vitro*, the neurons exhibited extensive neurite formation, and were easily distinguished from surrounding cells by the presence of oval, phase-bright somata and by the morphology of their processes. The somal diameters of neurons used in these studies averaged 17 ± 5.7 μm (mean ± SD). All related experiments were routinely performed in sister cultures, and the results were replicated in cultures from later dissections.

"Ca^{2+} deregulation" is an indicator of impending neuronal death

To study the relationships between Ca^{2+} and neurotoxicity, we first developed a means to monitor both neuronal $[Ca^{2+}]_i$ and survivability throughout a neurotoxic insult. In contrast to approaches where neuronal loss is gauged at a single time following a neurotoxic challenge, our method permitted us to study associations between neuronal $[Ca^{2+}]_i$ dynamics and eventual survival outcome. Figure 1*A* shows that when spinal neurons were exposed to a 50 min challenge with 250 μM glutamate, $[Ca^{2+}]_i$ rose rapidly, and then decayed to a lower "plateau." Following termination of the challenge, $[Ca^{2+}]_i$ in surviving neurons remained at the new plateau, or returned toward basal levels. However, many neurons underwent a delayed, sustained, and generally irreversible rise in $[Ca^{2+}]_i$ that often exceeded the dynamic range of the Ca^{2+} indicator (asterisks in Fig. 1*A*). This phenomenon closely paralleled neuronal staining with the vital dye trypan blue (Fig. 1*B*, Table 1), indicating that it must have preceded—or coincided with—neuronal death. Our observations in spinal neurons are in agreement with the recently reported observation that glutamate-induced $[Ca^{2+}]_i$ transients can trigger delayed Ca^{2+} overload and neurotoxicity in hippocampal neurons following single (Randall and Thayer, 1992) or repeated (Glaum et al., 1990) challenges. We named this phenomenon "Ca^{2+} deregulation," because following its onset, it could not be arrested by blocking Ca^{2+} channels with the dihydropyridine (DHP) nimodipine (1 μM), or by blocking NMDA receptors with DL-2-amino-5-phosphonovaleric acid (APV; 50 μM; data not shown). Also, it was not immediately reversible in some neurons by switching to a zero-Ca^{2+} buffer (data not shown), indicating that this secondary rise in $[Ca^{2+}]_i$ did not result from nonspecific plasma membrane leakiness, but more likely from a failure of cellular Ca^{2+} homeostatic mechanisms.

The process of Ca^{2+} deregulation was usually followed by positive staining with trypan blue or with ethidium homodimer, and lasted for up to 30–40 min before membrane lysis as judged by the loss of intracellular fura-2 fluorescence. This supports further the notion that secondary Ca^{2+} overload precedes severe damage to the neuronal membrane. Thus, in experiments where trypan blue was applied immediately following a neurotoxic challenge (no recovery period in control solution), only 75 of the 108 neurons undergoing Ca^{2+} deregulation stained positively (69%; see Fig. 7*A*). However, in a series of 107 experiments where a glutamate (250 μM), kainate (100 μM), or NMDA (100 μM) challenge was followed by a 30 min return to control solution, 628 of 634 deregulated neurons (99%) stained positively with trypan blue, revealing virtually a 1:1 relationship between these phenomena (see Table 1, Fig. 10*B*). By contrast with trypan blue, neuronal viability assessment with ethidium homodimer fluorescence correlated poorly with Ca^{2+} deregulation (Table 1) and grossly underestimated the fraction of cells stained with trypan blue both in spinal explant and in dissociated cultures. We were unable to improve the sensitivity of this assay with different concentrations (0.5–10 μM) of—or incubation times (10–30 min) with—ethidium homodimer. We did not attempt to examine neuronal viability with this marker at times exceeding 60 min beyond the termination of the glutamate challenge.

Glutamate neurotoxicity is a function of transmembrane Ca^{2+} gradient and of glutamate challenge duration

In our experiments, the glutamate challenge (250 μM L-glutamate for 50 min) caused both $[Ca^{2+}]_i$ increases and neuronal death (Fig. 1*A*). We asked whether the toxicity of glutamate (79.6 ± 13% trypan blue staining) was triggered by Ca^{2+} influx, or wheth-

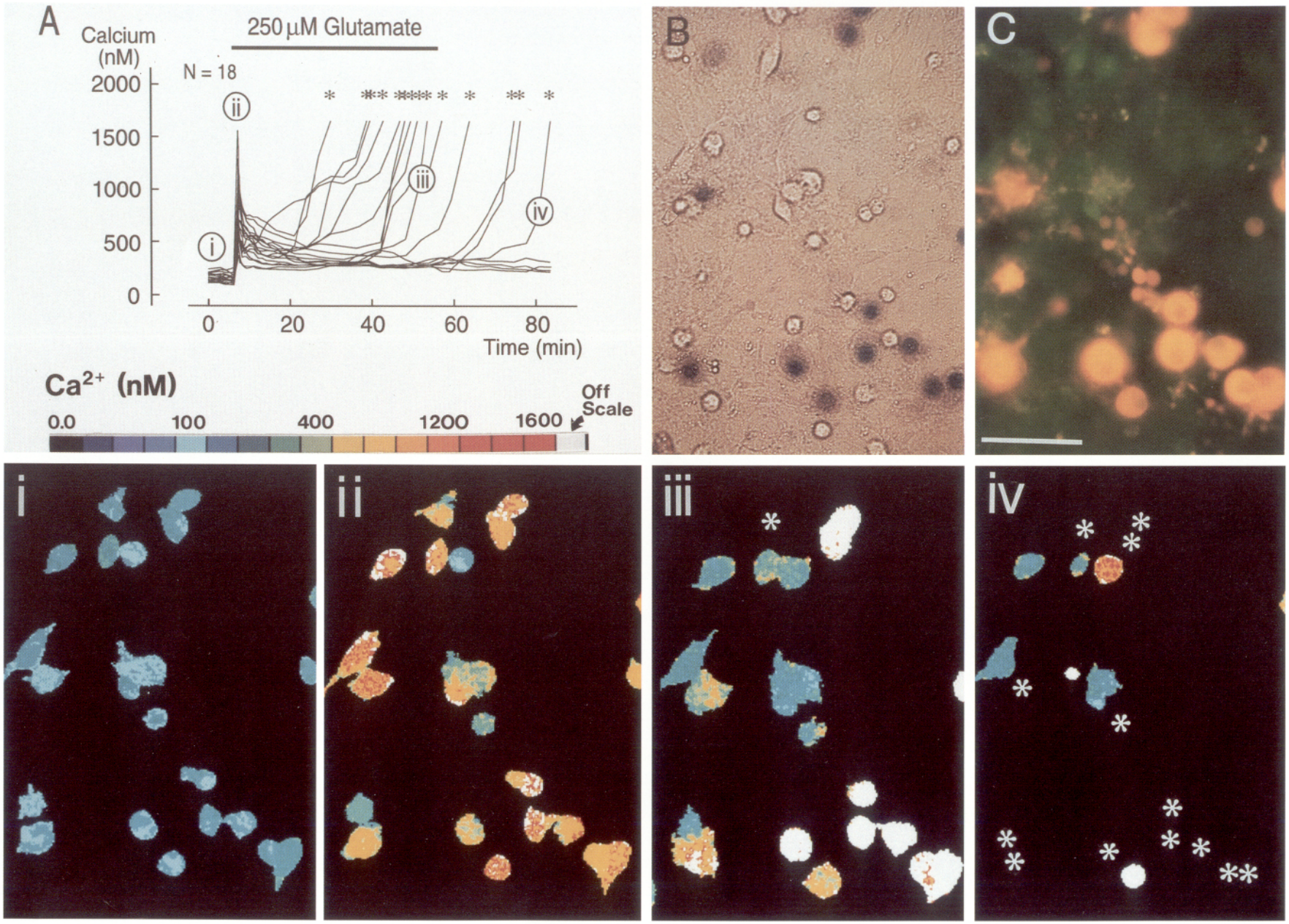

Figure 1. Time course of Ca^{2+} deregulation and assessment of neuronal death. *A,* Superimposed tracings of changes in $[Ca^{2+}]_i$ in 18 of the neurons shown in *i–iv*. Glutamate (250 μM) was bath applied for 50 min (*horizontal bar*), causing Ca^{2+} deregulation in 14 of 18 neurons. The tracings were truncated for the purpose of clarity whenever $[Ca^{2+}]_i$ irreversibly exceeded about 1700 nM (*asterisks*). *i-iv,* Calibrated fura-2 ratio images showing neuronal $[Ca^{2+}]_i$ at the times indicated in *A* (*i–iv*). Neurons undergoing Ca^{2+} deregulation sustained massive delayed elevations in $[Ca^{2+}]_i$ that often exceeded the dynamic range of the fluorescent indicator (*white neurons*). Ca^{2+} deregulation was sometimes followed by plasma membrane lysis and loss of fura-2 fluorescence (*asterisks*). The last $[Ca^{2+}]_i$ image (*iv*) reflects the extent of neuronal death (compare with *B* and *C*). *B,* Bright-field view of the neurons in *A* following incubation with trypan blue. *C,* Fluorescence (FITC) view of the neurons in A following incubation with ethidium homodimer and calcein/AM. Scale bar, 50 μm for *A–C*.

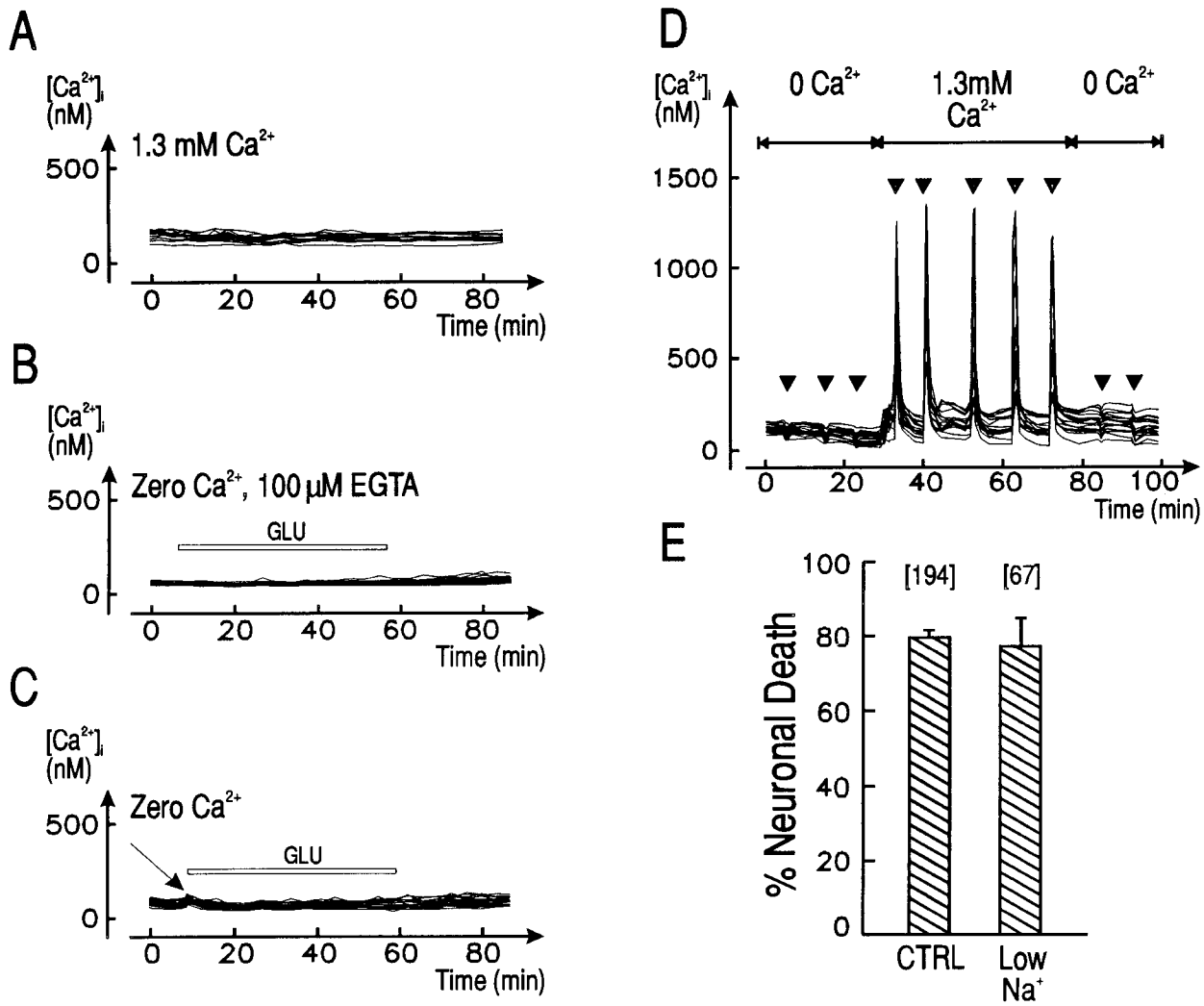

Figure 2. Dependence of glutamate-evoked $[Ca^{2+}]_i$ increases and neurotoxicity on extracellular Ca^{2+}. Each representative panel (*A–D*) shows the time course of $[Ca^{2+}]_i$ in several individual neurons in the same experiment. *A*, Control tracings from neurons in solution containing 1.3 mM Ca^{2+}, illustrating the stability of baseline $[Ca^{2+}]_i$ throughout the experiments (representative of three experiments). *B*, Effects of a 50 min challenge with 250 μM glutamate (*horizontal bar*) applied to neurons in Ca^{2+}-free solution containing 100 μM EGTA (representative of six experiments). *C*, Similar glutamate challenge applied to neurons in Ca^{2+}-free solution prepared without EGTA. Note brief rise in $[Ca^{2+}]_i$ at the challenge onset (*arrow*; representative of three experiments). *D*, Effects of brief (30 sec) applications of 200 μM glutamate (*triangles*) on $[Ca^{2+}]_i$ in neurons alternately perfused with solution containing 0 Ca^{2+} (and 100 μM EGTA) or 1.3 mM Ca^{2+}, illustrating the dependence of the glutamate-triggered $[Ca^{2+}]_i$ signal on extracellular Ca^{2+} (representative of five experiments). *E*, Ion substitution experiments performed in solution containing 1.3 mM $[Ca^{2+}]_e$, comparing the neurotoxicity of a 50 min glutamate challenge in control solution (*CTRL*; 130 mM NaCl, 1.3 mM $[Ca^{2+}]_e$) as compared with a low-Na^+ solution (130 mM choline-Cl iso-osmotically substituted for NaCl; 194 and 67 neurons in 13 and 5 experiments for control and low Na^+, respectively).

er it was caused by other, non-Ca^{2+} influx-dependent cytotoxic processes coactivated in parallel with—but independently of—Ca^{2+} influx.

In the absence of glutamate, $[Ca^{2+}]_i$ remained at basal levels throughout the period of study, illustrating the stability of the recordings (Fig. 2*A*). Figure 2*B* shows that when neurons were perfused in solution containing zero Ca^{2+} and 100 μM EGTA, baseline $[Ca^{2+}]_i$ dropped from about 100 nM to 50–60 nM (compare with Fig. 2*A*), but glutamate failed to trigger either $[Ca^{2+}]_i$ increases or neurotoxicity (six experiments, 53 neurons). These results were a consequence of extracellular Ca^{2+} removal, and not of other actions of EGTA (such as the induction of additional membrane conductances and membrane depolarization; Kauppinen et al., 1986), because similar results were obtained in three experiments repeated in zero Ca^{2+} without EGTA, apart from a modest brief rise in $[Ca^{2+}]_i$ at the start of the glutamate challenge (Fig. 2*C*). Neurons never underwent Ca^{2+} deregulation, and never stained with trypan blue in the absence of extracellular Ca^{2+}. These data confirm previous reports that extracellular Ca^{2+} is necessary to trigger the events leading to delayed Ca^{2+} overload and neuronal death (Choi, 1985; Garthwaite et al., 1986; Choi et al., 1987; Thayer and Miller, 1990).

Glutamate might also evoke a rise in $[Ca^{2+}]_i$ independently of Ca^{2+} influx. This could occur by activating intracellular cascades linked to the metabotropic receptor that, unlike the ionotropic glutamate receptors, is not linked to an ion channel (Farooqui and Horrocks, 1991; Opitz and Reymann, 1991). Could this alternate pathway cause the observed neurotoxicity by Ca^{2+} release from intracellular stores, rather than by the influx of extracellular Ca^{2+} (Frandsen and Schousboe, 1991)? Our results are contrary to this hypothesis, because $[Ca^{2+}]_i$ release was not observed following glutamate application in zero

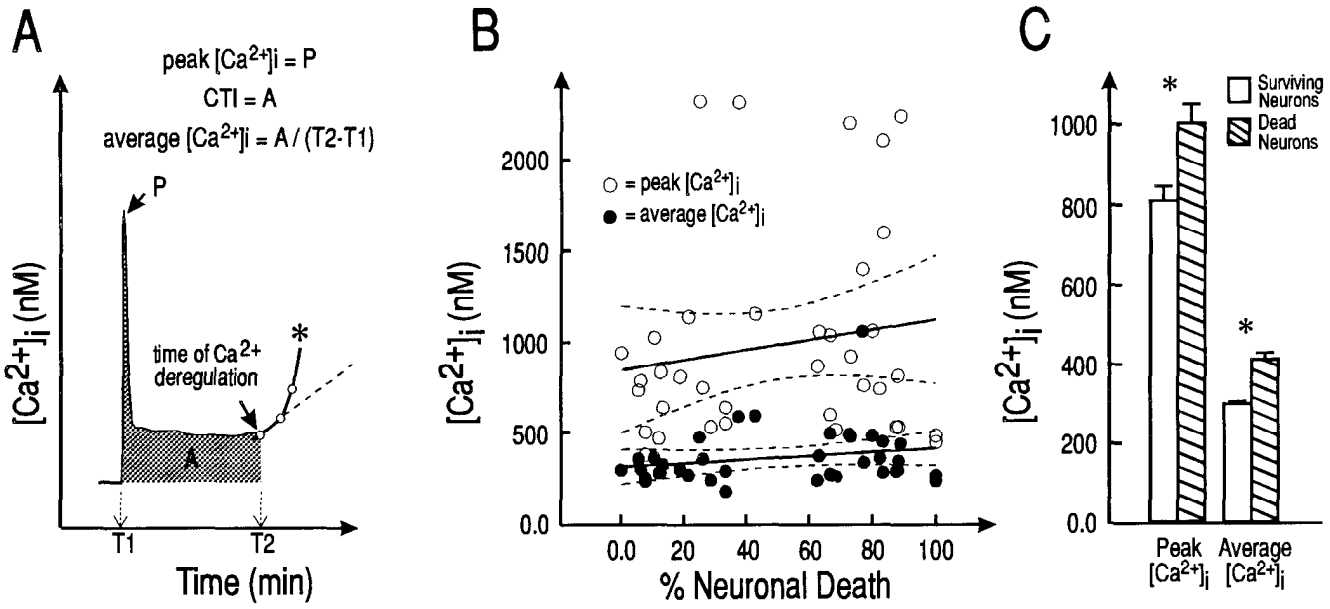

Figure 3. Lack of a simple predictive relationship between $[Ca^{2+}]_i$ parameters and neuronal death. *A*, Definition of peak $[Ca^{2+}]_i$, average $[Ca^{2+}]_i$, and CTI. The time of Ca^{2+} deregulation (*arrowed*) was defined by the point at which the slope of the $[Ca^{2+}]_i$ tracing became positive (*broken line*) for at least three consecutive $[Ca^{2+}]_i$ measurements (*circles*). *B*, Relationship between $[Ca^{2+}]_i$ and neuronal death at a fixed extracellular calcium concentration (1.3 mM). The rise in $[Ca^{2+}]_i$ was evoked by a 50 min challenge with either 250 μM glutamate, 100 μM NMDA, or 100 μM kainate. The fraction of trypan blue–stained neurons observed in each of 37 experiments is plotted against peak and average $[Ca^{2+}]_i$ for that experiment (*open* and *solid circles*, respectively). Both correlated poorly with neuronal death ($R = 0.16$ and $R = 0.21$, respectively). The *solid* and *broken lines show the best-fit least-squares straight lines and their 95% confidence intervals, respectively. C*, Analysis of the individual neurons in all the experiments in *B* showing that neurons that eventually died experienced, on average, greater elevations of $[Ca^{2+}]_i$ than neurons that survived ($n = 553$ neurons; *asterisks*, $p < 0.001$).

Ca^{2+} (Fig. 2*B,C*). In fact, Ca^{2+} influx was essential for triggering measurable glutamate-evoked and high K^+–evoked increases in $[Ca^{2+}]_i$ (Fig. 2*D*, representative of five experiments; similar records were obtained with 50 mM K^+ in three experiments). These results cannot exclude a neurotoxic contribution from Ca^{2+} sequestered in internal stores, but establish that its release would have to be triggered by Ca^{2+} influx (as in Ca^{2+}-induced Ca^{2+} release; Hernandez-Cruz et al., 1990; Miller, 1992).

Neurotoxicity has also been shown in some systems to occur through toxic alterations in the intracellular ionic environment due to depolarization-induced influx of Na^+ accompanied by Cl^- and water, leading to osmotic swelling and cell lysis (Rothman, 1985; Olney et al., 1986; Rothman and Olney, 1986). Figure 2*E* shows that this mechanism may be less important in spinal neurons: when 130 mM choline-Cl was substituted for NaCl in the control buffer (low Na^+, 1.3 mM Ca^{2+}), the toxicity of a 50 min challenge with 250 μM glutamate remained unchanged. These results are in agreement with those of Regan and Choi (1991) in a similar tissue culture system.

These experiments establish the necessity for Ca^{2+} influx in the mechanisms leading to early glutamate neurotoxicity in spinal neurons. However, they fail to explain the inability of intracellular Ca^{2+} measurements in some studies to predict the likelihood of neuronal death (Michaels and Rothman, 1990; Dubinsky and Rothman, 1991; Randall and Thayer, 1992). Figure 3*B* confirms that the same problem occurred in our experiments: when cultures were challenged with varying Ca^{2+} loads using 50 min challenges with different EAA receptor agonists (glutamate, NMDA, and kainate), the fraction of dead neurons per culture did not correlate with the mean values of peak or average $[Ca^{2+}]_i$ recorded in the neurons in the same experiment. However, both peak $[Ca^{2+}]_i$ and average $[Ca^{2+}]_i$ were found to have been more elevated in individual neurons that died as compared with those that survived (Fig. 3*C*).

The lack of a predictive relationship between $[Ca^{2+}]_i$ and neurotoxicity may be due to nonlinearities in intracellular $[Ca^{2+}]_i$ dynamics (see below), or due to inadequacies in the temporal and/or spatial discrimination ability of the $[Ca^{2+}]_i$ measurement technique (e.g., inability to resolve subcellular $[Ca^{2+}]_i$ transients). To examine these possibilities, we studied the impact of a fixed glutamate challenge on $[Ca^{2+}]_i$ and survivability, while varying the concentrations of extracellular Ca^{2+} ($[Ca^{2+}]_e$; 0–10 mM). According to the Goldman-Hodgkin-Katz current equation (Hille, 1992), Ca^{2+} flux through an open ionic channel should vary as a function of $[Ca^{2+}]_e$. Therefore, during a glutamate challenge, submembrane $[Ca^{2+}]_i$ would be determined

→

Figure 4. Dependence of glutamate neurotoxicity on transmembrane Ca^{2+} gradient and on challenge duration. Neurons were perfused with solutions containing varying concentrations of Ca^{2+}, and exposed to a 250 μM glutamate challenge (*GLU*). *A*, Relationship between $[Ca^{2+}]_e$ and neuronal death gauged with trypan blue. *B*, Relationship between $[Ca^{2+}]_e$, peak $[Ca^{2+}]_i$, and average $[Ca^{2+}]_i$ (see Materials and Methods and Fig. 3*A* for definitions) evoked by the glutamate challenge. In *A* and *B*, each symbol represents a mean value taken from five experiments performed at the same $[Ca^{2+}]_e$ (7–16 neurons per experiment). SEs are shown where they exceed the symbol size. To determine half-maximal $[Ca^{2+}]_e$ (EC_{50}) values (*broken lines*), the algorithm of Marquardt (1963) was used to fit the data to the equation $\text{effect}/\text{effect}_{max} = [Ca^{2+}]_e/(EC_{50} + [Ca^{2+}]_e)$ (*solid lines*). *C–E*, Representative effects of 50 min glutamate (*horizontal bar*) on $[Ca^{2+}]_i$ in neurons perfused with solutions containing 0.3, 1.3, and 10

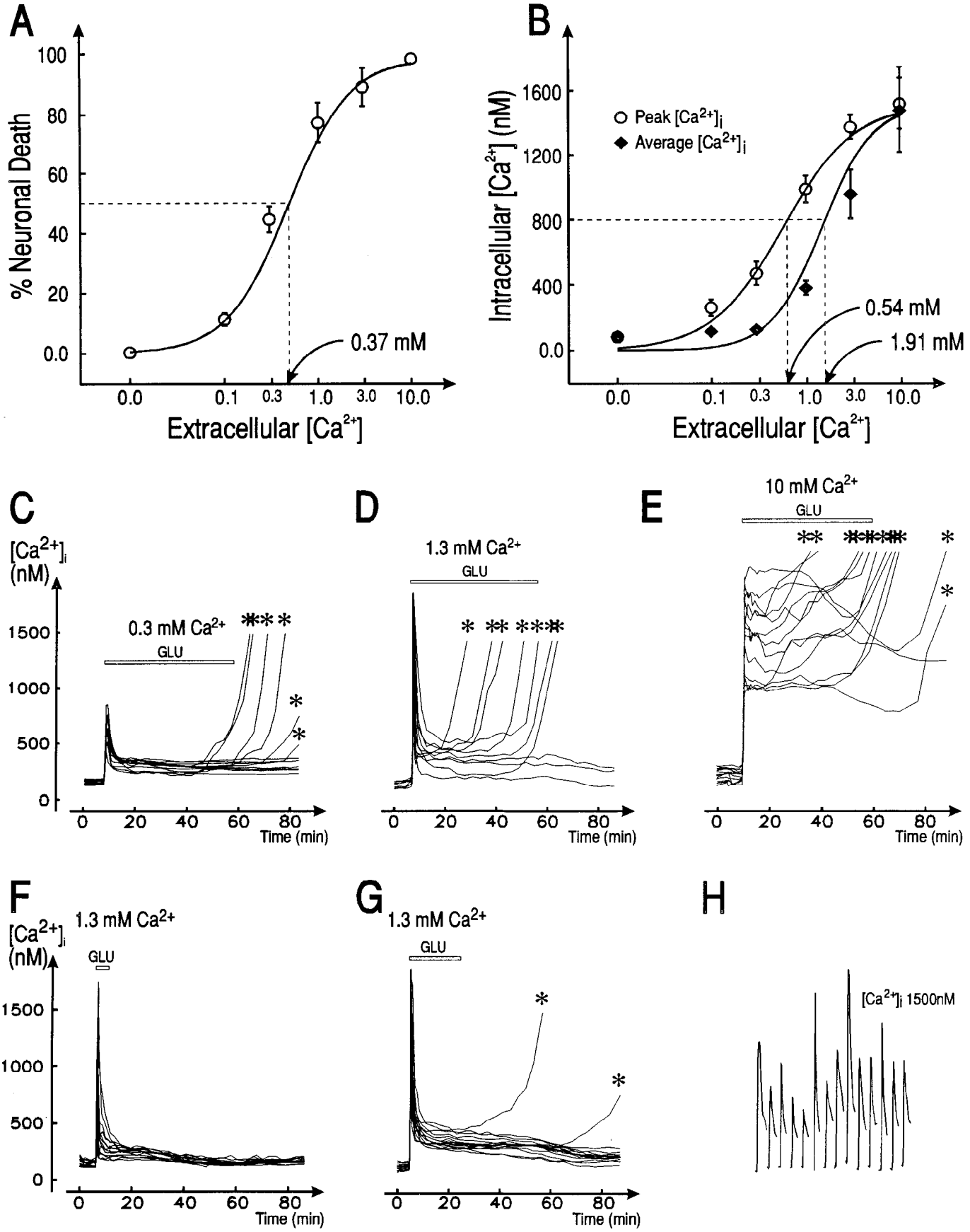

mM Ca^{2+}, respectively. *F–G*, Representative effects of shorter glutamate challenges (5 and 15 min, respectively) on $[Ca^{2+}]_i$ in neurons perfused with 1.3 mM $[Ca^{2+}]_e$ (compare with *D*). The *asterisks* in *C–G* denote Ca^{2+} deregulations. *H*, Staggered view of the primary $[Ca^{2+}]_i$ transients evoked in the 14 neurons in *G*, illustrating the variability of peak $[Ca^{2+}]_i$ responses in a typical experiment.

Table 2. Relationship between glutamate challenge duration and neuronal death

Exposure time	No. of experiments	No. of neurons	% Ca^{2+} deregulations	% trypan blue positive
5 min	5	42	4.70 ± 0.26*	4.70 ± 0.26*
15 min	5	53	17.0 ± 1.20*	17.0 ± 1.20*
50 min	13	194	77.8 ± 2.98*	79.6 ± 1.32*

Effects of 5, 15, and 50 min challenges with 250 μM glutamate on neuronal death gauged by Ca^{2+} deregulations and by staining with trypan blue.

* $p < 0.001$ versus both other time groups.

by the permeability and gating characteristics of the ionic channels involved. In this instance, increasing $[Ca^{2+}]_e$ would cause submembrane $[Ca^{2+}]_i$ to increase, irrespective of the ability of the Ca^{2+} measurement apparatus to resolve the fact (Swandulla et al., 1991). This paradigm allowed us to compare the neurotoxic effects of different neuronal Ca^{2+} loads without relying on $[Ca^{2+}]_i$ measurements. In addition, this strategy isolates the neurotoxic effects of Ca^{2+}, because by keeping the glutamate challenge unchanged, the impact of any Ca^{2+} influx–independent glutamate-activated neurotoxic processes would remain unaltered.

In the experiments presented in Figure 4*A–E*, we found a sigmoidal concentration–response relationship between $[Ca^{2+}]_e$ and neuronal death (Fig. 4*A*; slope of 1.28 ± 0.11 on a probit plot). This shows that as the transmembrane Ca^{2+} gradient increased, a higher proportion of neurons stained with trypan blue. Therefore, the likelihood of reaching the neurotoxicity threshold was dependent on submembrane $[Ca^{2+}]_i$. However, despite the clear relationship between $[Ca^{2+}]_e$ and cell death, the $[Ca^{2+}]_e$ increases did not produce proportional changes in measured peak $[Ca^{2+}]_i$ or average $[Ca^{2+}]_i$ (Fig. 4*B*; representative experiments are shown in Fig. 4*C–E*). For example, a 10-fold increase in $[Ca^{2+}]_e$ from 1 mM to 10 mM only increased peak $[Ca^{2+}]_i$ 1.53-fold. The insensitivity of the change in $[Ca^{2+}]_i$, particularly in the range of $[Ca^{2+}]_e$ that produced a high probability of cell death, partly explains the inability of linear correlations to confirm any significant relationships between $[Ca^{2+}]_i$ and neuronal survival outcome. The inability of measured $[Ca^{2+}]_i$ to reflect the changes in $[Ca^{2+}]_e$ can be explained by one or more of four mechanisms. First, as $[Ca^{2+}]_i$ rises in the cytoplasm, it approaches the concentration range at which cytosolic Ca^{2+} buffering proteins are maximally effective. Therefore, there is a "ceiling" on the rise in $[Ca^{2+}]_i$ because $[Ca^{2+}]_i$ transients are buffered more effectively at higher Ca^{2+} loads (Thayer and Miller, 1990; Artalejo et al., 1992). Second, Ca^{2+} influx may saturate at higher transmembrane Ca^{2+} gradients (Hille, 1992). Third, $[Ca^{2+}]_i$ may only rise in restricted subcellular compartments, and thus may be registered at a lower level when imaged $[Ca^{2+}]_i$ is averaged both spatially and temporally throughout the entire cell soma as was done in the present experiments. Fourth, as $[Ca^{2+}]_i$ increases to micromolar levels (Fig. 4*B*), it may approach the saturation limits of the Ca^{2+} indicator. This was most likely to occur in experiments where $[Ca^{2+}]_e$ was set at 10 mM (Fig. 4*E*). We note, however, that fura-2 has been used with reasonable accuracy to measure Ca^{2+} concentrations in the 1500 nM range (Roe et al., 1990; Guthrie et al., 1991; Muller and Connor, 1991). In the majority of our experiments (performed in 1.3 mM Ca^{2+}), $[Ca^{2+}]_i$ only exceeded this range in a small fraction of neurons (e.g., Fig. 4*H*). Thus, saturation of fura-2 was unlikely to bias our $[Ca^{2+}]_i$ measurements significantly when $[Ca^{2+}]_e$ was in the 0–1.3 mM range. The $[Ca^{2+}]_i$ values in the present report are similar to those obtained by others in analogous experiments performed with the indicator indo-1 (Randall and Thayer, 1992).

The duration of the glutamate challenge influenced the probability of neuronal death. When neurons were exposed to glutamate for varying periods, both the frequency of Ca^{2+} deregulations, and trypan blue staining (cell death) increased with longer challenge durations (compare Fig. 4*D,F,G*; Table 2). This result, taken in the context of the findings in Figure 4*A*, suggests that Ca^{2+} neurotoxicity depends both on $[Ca^{2+}]_i$ and on the duration of the Ca^{2+} load. Recently, Randall and Thayer (1992) showed in hippocampal neurons that a 5 min exposure to 100 μM glutamate sufficed to trigger delayed Ca^{2+} overload over periods ranging from 0 to 3 hr. Our data support this finding, and add that in spinal neurons, the mechanisms leading to toxicity continue to be triggered throughout the glutamate exposure despite the fact that measured $[Ca^{2+}]_i$ declines to a lower steady-state level within minutes of the onset of the primary $[Ca^{2+}]_i$ rise. This steady-state $[Ca^{2+}]_i$ plateau likely consists of a dynamic balance between ongoing Ca^{2+} influx through residual noninactivated pathways and Ca^{2+} efflux or buffering, because the plateau level could be lowered or raised by switching to solutions containing zero Ca^{2+} or 10 mM calcium, respectively (data not shown).

Ca^{2+}-triggered neurotoxicity is source specific

Is all Ca^{2+} equally neurotoxic? If so, then neuronal death should depend solely on the magnitude and the time course of the $[Ca^{2+}]_i$ rise, rather than on its source. Previous reports indicated that Ca^{2+} influx through voltage-sensitive Ca^{2+} channels and glutamate receptor–operated channels can be evoked independently (Mayer et al., 1987; Murphy et al., 1987; Holopainen et al., 1989; Yuste and Katz, 1991). We asked whether a rise in $[Ca^{2+}]_i$ mediated through these different pathways would cause equal neurotoxicity. To examine the independence of glutamate- and depolarization-mediated Ca^{2+} influx, we exposed neurons in explant cultures to brief applications (30 sec) of high K^+ (50 mM) and of glutamate (250 μM), both of which evoked large $[Ca^{2+}]_i$ transients. Figure 5 and the accompanying images in Figure 6 show that in our preparation, $[Ca^{2+}]_i$ transients produced by glutamate and high K^+ contain significant independent components: nimodipine (1 μM), a blocker of L-type voltage-gated Ca^{2+} channels, substantially attenuated $[Ca^{2+}]_i$ transients evoked by high K^+, but had no significant effect on the rise in $[Ca^{2+}]_i$ evoked by glutamate. To attenuate the latter, a combination of the NMDA antagonist APV (50 μM) and the non-NMDA antagonist CNQX (75 μM; Honore et al., 1988) was required. Figure 5*B* illustrates that the K^+-evoked transients were primarily DHP sensitive and were not composed of fractions sensitive to glutamate receptor antagonists (APV + CNQX)

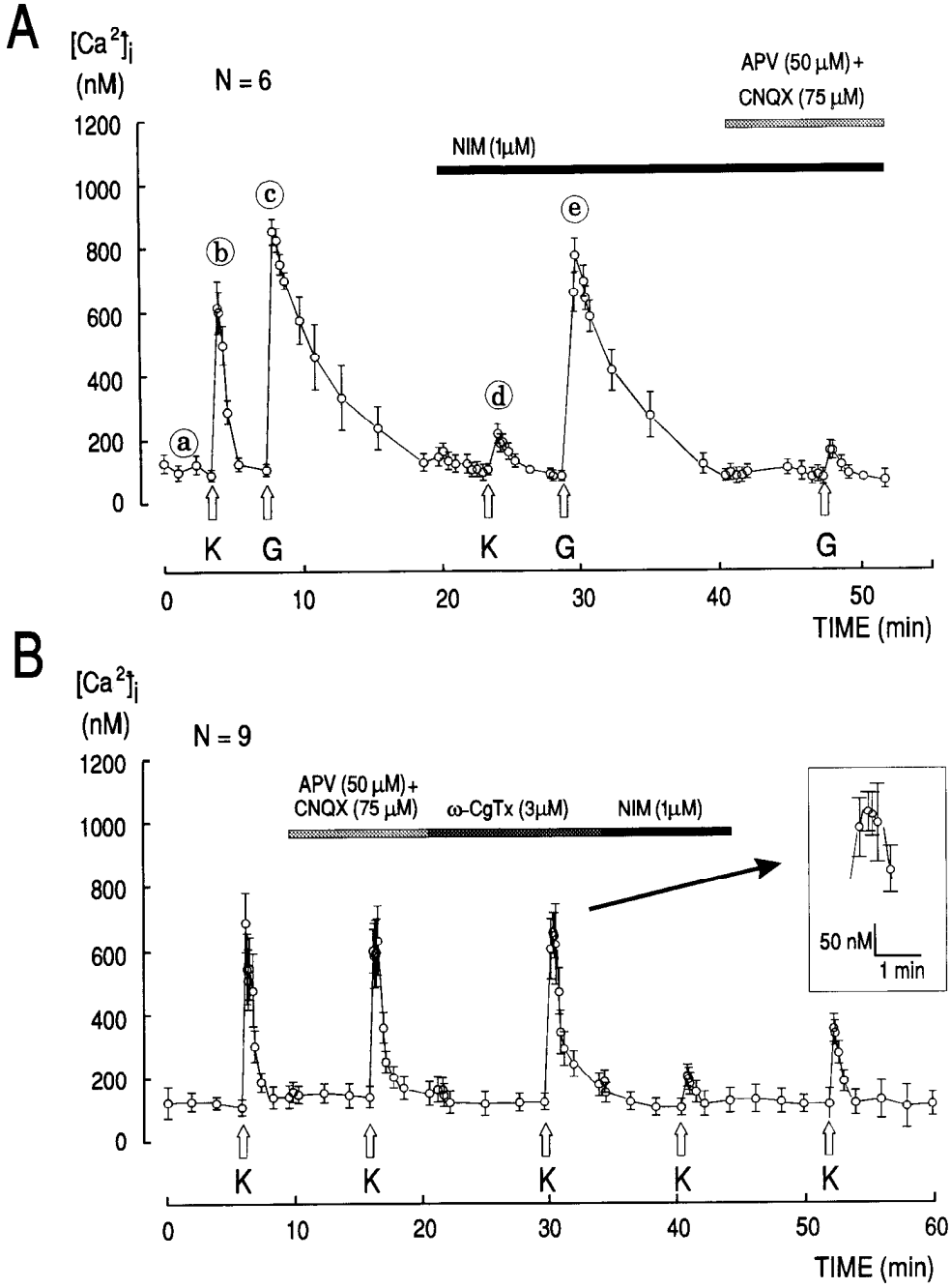

Figure 5. Characterization $[Ca^{2+}]_i$ transients evoked by brief (30 sec) applications (*arrows*) of 250 μM glutamate (*G*) and 50 mM potassium (*K*) to neurons in explant cultures. Mean $[Ca^{2+}]_i$ responses from six and nine neurons (in *A* and *B*, respectively) are shown with their SEs. *A*, Independence of $[Ca^{2+}]_i$ transients evoked by potassium and by glutamate (representative of five experiments). Nimodipine (*NIM, solid bar*) attenuates the $[Ca^{2+}]_i$ transient evoked by depolarization with potassium, but has little effect on the glutamate-evoked transient. The latter was attenuated by APV and CNQX (50 μM and 75 μM, respectively; *gray bar*). In this experiment, recovery of the glutamate-evoked $[Ca^{2+}]_i$ transient was slower than recovery of the potassium-evoked transient, suggesting that glutamate and high K^+ may have different effects on neuronal Ca^{2+} regulation. The fura-2 ratio images displayed in Figure 6 correspond to the times indicated (*a–e*). *B*, Further characterization of the K^+-evoked $[Ca^{2+}]_i$ transients (representative of five experiments), which were unaffected by APV and CNQX (*light gray bar*) or ω-conotoxin GVIA (*ω-CgTx, dark gray bar*). As in *A*, the K^+-evoked $[Ca^{2+}]_i$ transient was mostly (about 80%) blocked by nimodipine (*solid bar*), leaving a fraction resistant to DHPs, ω-conotoxin, and glutamate receptor antagonists. *Inset*, Peak of third K^+-evoked $[Ca^{2+}]_i$ transient with magnified time scale showing that $[Ca^{2+}]_i$ remains at a maximum for approximately 15–20 sec, during which three or four separate $[Ca^{2+}]_i$ measurements were performed.

or to ω-conotoxin GVIA, a blocker of N-type Ca^{2+} channels. The residual, DHP-insensitive $[Ca^{2+}]_i$ transients were consistent with the presence of DHP- and ω-conotoxin-insensitive Ca^{2+} currents in neurons (Rosario et al., 1989; Regan et al., 1991; Scroggs and Fox, 1991).

If Ca^{2+} neurotoxicity were solely dependent on an excessive rise in $[Ca^{2+}]_i$, then equivalent $[Ca^{2+}]_i$ increases evoked by activating voltage-sensitive or glutamate-operated Ca^{2+}-permeable channels should produce equivalent amounts of neuronal death. Using spinal cord explants, we randomly allocated cultures to one of two groups. In one group, the neurons were superfused with 250 μM glutamate. In the other, neurons were superfused for the same duration with 50 mM potassium (high-K^+ group). The appropriate challenge duration and agonist concentrations were determined empirically in pilot experiments so as to elicit purposefully $[Ca^{2+}]_i$ changes of similar magnitudes and time courses in neurons of equal diameters from both groups (same peak and average $[Ca^{2+}]_i$; Fig. 7*A,B*). $[Ca^{2+}]_i$ was recorded in each neuron in the experimental field as shown in the representative experiments in Figure 7, *D* and *E*. Following the glutamate or high-K^+ challenge, neuronal death was assayed with trypan blue staining. To allow for the fact that neurotoxicity is also a function of Ca^{2+} challenge duration (Table 2), the CTI (Ca^{2+}–time index), a measure of total Ca^{2+} load over time, was determined for each neuron (see Materials and Methods for definition). Figure 7*C* illustrates that the total challenge-evoked Ca^{2+} load as determined by the CTI was significantly smaller for neurons exposed to glutamate as compared with high K^+ ($t = 9.06$, $p < 0.0001$).

Despite having elicited equivalent measurable $[Ca^{2+}]_i$ eleva-

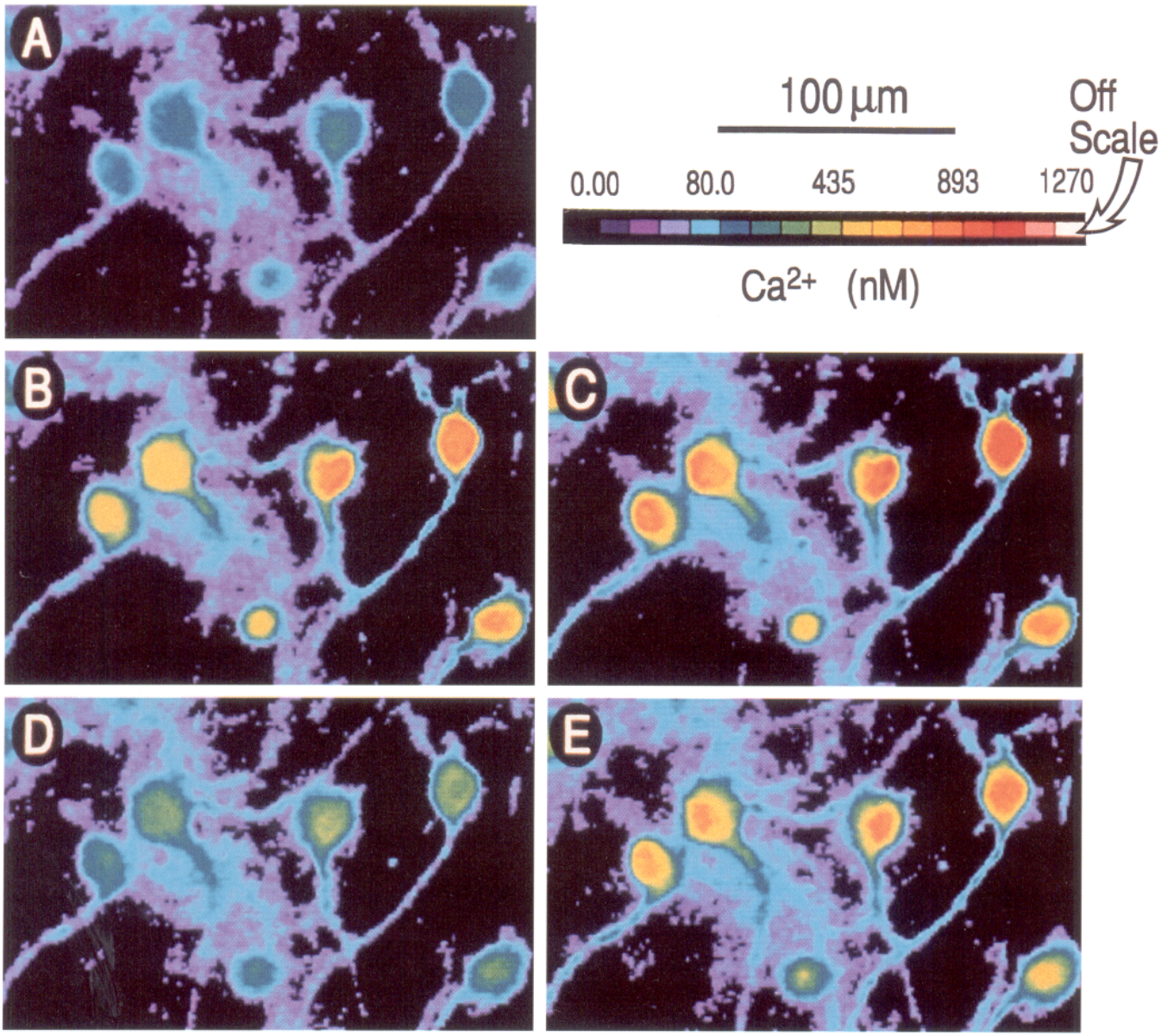

Figure 6. Calibrated fluorescence ratio images of $[Ca^{2+}]_i$ in the six spinal neurons for the times shown in Figure 5*A*. Due to the density of the explants, some background Ca^{2+} fluorescence is registered from supporting cells (glia, fibroblasts) in all panels. Note, however, that this background remains unchanged throughout the experiment.

tions in the high-K^+ and glutamate groups, and a lower total Ca^{2+} load (CTI) in the latter, more neurons died in the glutamate group (Figs. 7*D,E*; 8). Statistically, neurons exposed to glutamate had a dramatically higher probability of undergoing Ca^{2+} deregulation ($t = 8.25$, $p < 0.0001$) and of dying ($t = 6.64$, $p < 0.0001$). A survival analysis of the time course of Ca^{2+} deregulation (Kaplan–Meier survival model; see section 14.5 in Armitage and Berry, 1987) confirmed that in neurons exposed to glutamate, Ca^{2+} deregulation occurred sooner and to a greater extent than with high K^+ (log-rank $\chi^2 = 58.44$, $p < 0.0001$; Fig. 8*B*). We interpret these results as reflecting a difference in the mechanism by which Ca^{2+} triggers neurotoxicity, rather than a difference in the ability of high K^+ and glutamate to trigger non-Ca^{2+}-dependent neurotoxic phenomena. This is because high K^+ was unlikely to trigger any significant neurotoxic cascades (Fig. 8*A*), whereas in the case of glutamate, neurotoxicity did not depend on the influx of Na^+ (Fig. 2*E*), and was absolutely dependent on Ca^{2+} influx (Figs. 2*B,C*; 4*A*). Thus, our data demonstrate quantitatively that all sustained elevations in $[Ca^{2+}]_i$ are not equally neurotoxic, as the toxicity clearly also depends on the source of Ca^{2+} influx.

Glutamate-mediated neurotoxicity is Ca^{2+} source specific

Glutamate activates a variety of receptor subtypes (for reviews, see Dingledine et al., 1988; Watkins et al., 1990; Zorumski and Thio, 1992), all of which have been implicated in mediating neuronal death (e.g., Garthwaite and Garthwaite, 1983; Simon et al., 1984; Choi et al., 1987; Goldberg et al., 1987; Koh et al., 1990; Urca and Urca, 1990; Mosinger et al., 1991; Opitz and Reymann, 1991). Our results and those of others (e.g., Choi,

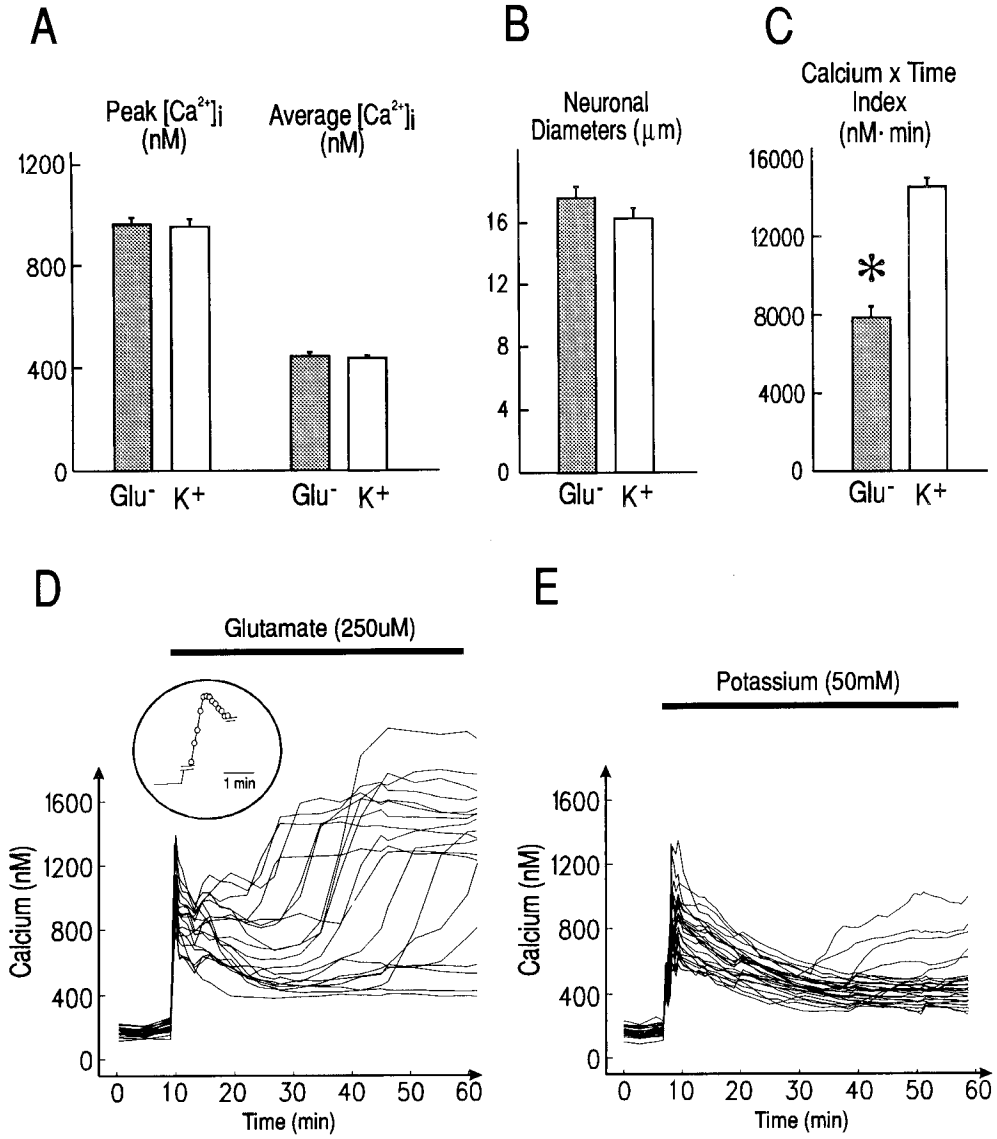

Figure 7. Comparison of measures of Ca^{2+} load experienced by neurons exposed to 50 min challenges with 250 μM glutamate (*GLU*; 109 neurons in 12 experiments) or with 50 mM potassium (high K^+; 85 neurons in 10 experiments). Peak $[Ca^{2+}]_i$, average $[Ca^{2+}]_i$, and CTI were calculated as described in Materials and Methods. Statistical differences (*asterisk*) were taken at the $p = 0.05$ level. *A*, The glutamate and high-K^+ challenges evoked the same peak and same average $[Ca^{2+}]_i$ rise. *B*, The neuronal diameters were comparable in both groups. *C*, The CTI, a measure of total Ca^{2+} load over time, was significantly less for the glutamate group. *D*, Representative experiment showing that glutamate-evoked $[Ca^{2+}]_i$ transients were frequently followed by a large number of early Ca^{2+} deregulations. *Inset*, Magnified time scale tracing showing the peak of a single glutamate-evoked $[Ca^{2+}]_i$ transient. The peaks typically lasted 15–20 sec, allowing sufficient time for several fluorescence ratio measurements (*open circles*). *E*, Representative experiment showing that $[Ca^{2+}]_i$ transients evoked by high K^+ produced far fewer Ca^{2+} deregulations than those evoked by glutamate.

1985, 1987; Murphy et al., 1988) implicate Ca^{2+} influx as a chief mediator of glutamate neurotoxicity. However, the relative contribution of the different receptor subtypes to neurotoxicity remains unclear. Is the neurotoxicity mediated by a given Ca^{2+} influx path (e.g., NMDA receptor–operated channels) solely a function of that path's ability to cause excessive increases in $[Ca^{2+}]_i$? Conversely, given equivalent Ca^{2+} influx–mediated $[Ca^{2+}]_i$ increases, are all glutamate receptor subtypes equally capable of triggering neurotoxicity? To address this issue we dissected pharmacologically the pathways of glutamate-evoked Ca^{2+} elevations in spinal neurons. Agonists and antagonists of Ca^{2+} channels and glutamate receptors were applied to neurons in dissociated cultures at concentrations chosen to evoke similar elevations in neuronal $[Ca^{2+}]_i$ parameters (peak and average $[Ca^{2+}]_i$), but by different routes. The neurons were challenged for 50 min with glutamate (250 μM), NMDA (100 μM), or kainate (100 μM) in the presence of varying combinations of APV (50 μM), nimodipine (1 μM), or CNQX (75 μM). The exposure was followed by a 30 min return to control solution that also contained the antagonist combination. $[Ca^{2+}]_i$, its time course, and the survival outcomes were monitored in all neurons ($n = 553$), and the data used for statistical modeling of the relationships between neuronal survival, route of Ca^{2+} influx, and the measured Ca^{2+} parameters. Representative experiments and the summary data are shown in Figures 9 and 10 and in Table 3.

In the presence of NMDA receptor blockade (Fig. 9*A*), the glutamate challenge still elicited a $[Ca^{2+}]_i$ transient of comparable amplitude (peak $[Ca^{2+}]_i$) to that evoked by glutamate alone (Fig. 9*A*; compare with Figs. 1*A*, 4*D*). However, despite the large rise in $[Ca^{2+}]_i$, only one neuron underwent deregulation (Fig. 9*A*, asterisk). The glutamate-evoked Ca^{2+} influx was not mediated to any significant extent by DHP-sensitive Ca^{2+} channels, because the $[Ca^{2+}]_i$ transient was not significantly attenuated by nimodipine (Figs. 9*B*, 10*A*; see also experiments in Figs. 5, 6). Figure 9*C* illustrates that in the presence of APV, the glutamate-mediated rise in $[Ca^{2+}]_i$ was mediated primarily by non-NMDA channels sensitive to CNQX, as this agent almost completely attenuated the $[Ca^{2+}]_i$ transient. The residual rise in $[Ca^{2+}]_i$ observed in Figure 9*C* may be due to incomplete blockade of all glutamate receptors, but is unlikely to represent phosphoinositide-mediated internal Ca^{2+} release through metabotropic receptor activation because this was not seen in the absence of extracellular Ca^{2+} (Fig. 2*B,C*). The experiments in Figures 9*A–C* indicate that glutamate neurotoxicity was uncommon when

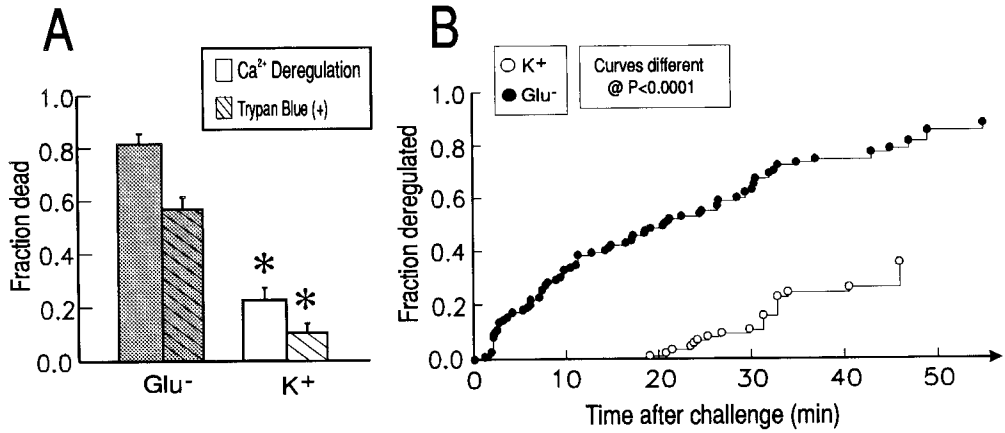

Figure 8. Survival analyses of the neurons in Figure 7*A–C* showing that equivalent neuronal Ca^{2+} loads triggered by different sources produce significantly different degrees of neurotoxicity. *A*, Comparison of the fraction of neurons staining positively with trypan blue (*hatched bars*) or undergoing Ca^{2+} deregulations (*open bars*) in each group. *Asterisks* denote statistical differences at $p < 0.0001$. *B*, Kaplan–Meier survival plot showing the fraction of Ca^{2+} deregulations in each group as a function of time. Neurons exposed to glutamate (*solid circles*) underwent earlier, more frequent Ca^{2+} deregulations than those exposed to high K^+ (*open circles*).

NMDA channels were blocked. More importantly, they show quantitatively that a large rise in $[Ca^{2+}]_i$ was not in itself sufficient to cause much neurotoxicity for the duration of these experiments, and that the non-neurotoxic $[Ca^{2+}]_i$ transient seen in Figure 9, *A* and *B*, consisted of that fraction that was CNQX sensitive. These results are analogous to the findings by Dubinsky and Rothman (1991) that in cultured hippocampal neurons, sodium cyanide produced large elevations in $[Ca^{2+}]_i$, but was not neurotoxic. The notion that certain elevations in $[Ca^{2+}]_i$ are not necessarily neurotoxic is strengthened further in Figure 9*D–F*: NMDA alone evoked a rise in $[Ca^{2+}]_i$ that was smaller in magnitude than that evoked with glutamate (Figs. 9*D*, 10*A*). However, despite producing a smaller $[Ca^{2+}]_i$ rise, the NMDA challenge caused most of the neurons to undergo Ca^{2+} deregulation (asterisks). Kainate caused an equivalent rise in $[Ca^{2+}]_i$ to NMDA, but this was not accompanied by frequent cell death (Figs. 9*E*, 10*A,B*). To examine whether the difference between the neurotoxicity of NMDA and of kainate was a function of Ca^{2+} load, we pretreated the cultures for 1 hr with 50 μg/ml of concanavalin A. This maneuver reduces non-NMDA receptor desensitization in an irreversible manner (Mayer and Vyklicky, 1989). Figure 9*F* shows that this strategy increased the apparent area under the $[Ca^{2+}]_i$ time course curve (CTI) but did not result in increased neurotoxicity as compared with kainate alone (Fig. 10*B*). In comparing the neurotoxicity of the different Ca^{2+} sources (Fig. 10*B*), there was a striking difference in neuronal death between groups with and without NMDA receptor blockade, confirming that glutamate neurotoxicity was predominantly NMDA mediated, and was triggered by Ca^{2+} influx. Furthermore, this was not due to the ability of NMDA receptors to elicit higher measurable elevations in $[Ca^{2+}]_i$, because non-NMDA receptor activation elicited $[Ca^{2+}]_i$ increases of equal or greater magnitude than NMDA receptors alone (Fig. 10*A*).

In the experiments shown in Figures 3 and 4, we proposed that the lack of a predictive association between $[Ca^{2+}]_i$ and cell death may reflect in part nonlinear relationships between Ca^{2+} influx and measured $[Ca^{2+}]_i$. Here, given that all Ca^{2+} influx was not equally neurotoxic (Figs. 7–10), we examined the feasibility of uncovering the relationship between $[Ca^{2+}]_i$ and neuronal death by accounting for Ca^{2+} source specificity in our analysis. To this end, we used regression analysis to model the probability of Ca^{2+} deregulation as a function of calcium source, challenge duration, peak $[Ca^{2+}]_i$, average $[Ca^{2+}]_i$, and CTI (calcium–time index). The analysis tests the statistical significance, and the usefulness, of each of these parameters to the relationships described by the model. Two separate modeling strategies were employed: linear (multiple) regression and logistic regression, the latter being more widely accepted for fitting models to binary outcome variables (e.g., alive/dead; see Chaps. 10 and 12 in Armitage and Berry, 1987). Several regression models containing different parameter combinations were tested (Table 3). The importance of each parameter to predicting outcome was determined by comparing the goodness of fit of the different models to the observed probability of Ca^{2+} deregulation. Also, within each model, each parameter was tested for statistical significance with the others taken into account (e.g., significance of peak $[Ca^{2+}]_i$ given its source).

Table 3 shows that with both modeling strategies, there was a marked dependence of the goodness of fit of the model on the inclusion of the parameters calcium source and time to deregulation, but a much lesser dependence on peak $[Ca^{2+}]_i$, average $[Ca^{2+}]_i$, or CTI. Using linear regression, when either source or time was excluded, the goodness of fit of the models decreased considerably (R^2 reduced to 0.431 and 0.337 for source and time excluded, respectively). By comparison, goodness of fit was virtually unaffected by excluding the parameters of peak, average, or CTI (R^2 of 0.638 in the model with all parameters included, vs R^2 of 0.624 when only source and time were included). Similarly, using logistic regression, a perfect fit was obtained by including the parameters source, time, and peak $[Ca^{2+}]_i$ ($p = 1.0000$). The goodness of fit was essentially unaffected by excluding the parameter peak ($p = 0.9998$), but was grossly reduced if the Ca^{2+} source was excluded ($p = 0.0132$). These analyses demonstrate that Ca^{2+} source and time were the most

→

Figure 9. Representative experiments showing the method of pharmacological dissection of the route of neurotoxic $[Ca^{2+}]_i$ increase. Spinal neurons were exposed to a 50 min challenge with either 250 μM glutamate (*GLU*), 100 μM NMDA, or 100 μM kainate, in the presence or absence of specific antagonists of NMDA receptors (50 μM APV), non-NMDA receptors (75 μM CNQX), or L-type Ca^{2+} channels [1 μM nimodipine (*NIM*)]. Each challenge was followed by a 30 min recovery period. Neurotoxicity was gauged by Ca^{2+} deregulations (*asterisks*) and by trypan blue staining (see Fig. 10*B*). *A–C*, Challenges with glutamate in the presence of APV, APV plus nimodipine, and APV plus CNQX, respectively. *D*, challenge with NMDA without NMDA receptor blockade. *E*, Kainate challenge in the presence of APV and nimodipine. *F*, Kainate challenge as in *E* following pretreatment with concanavalin A (*CON-A*).

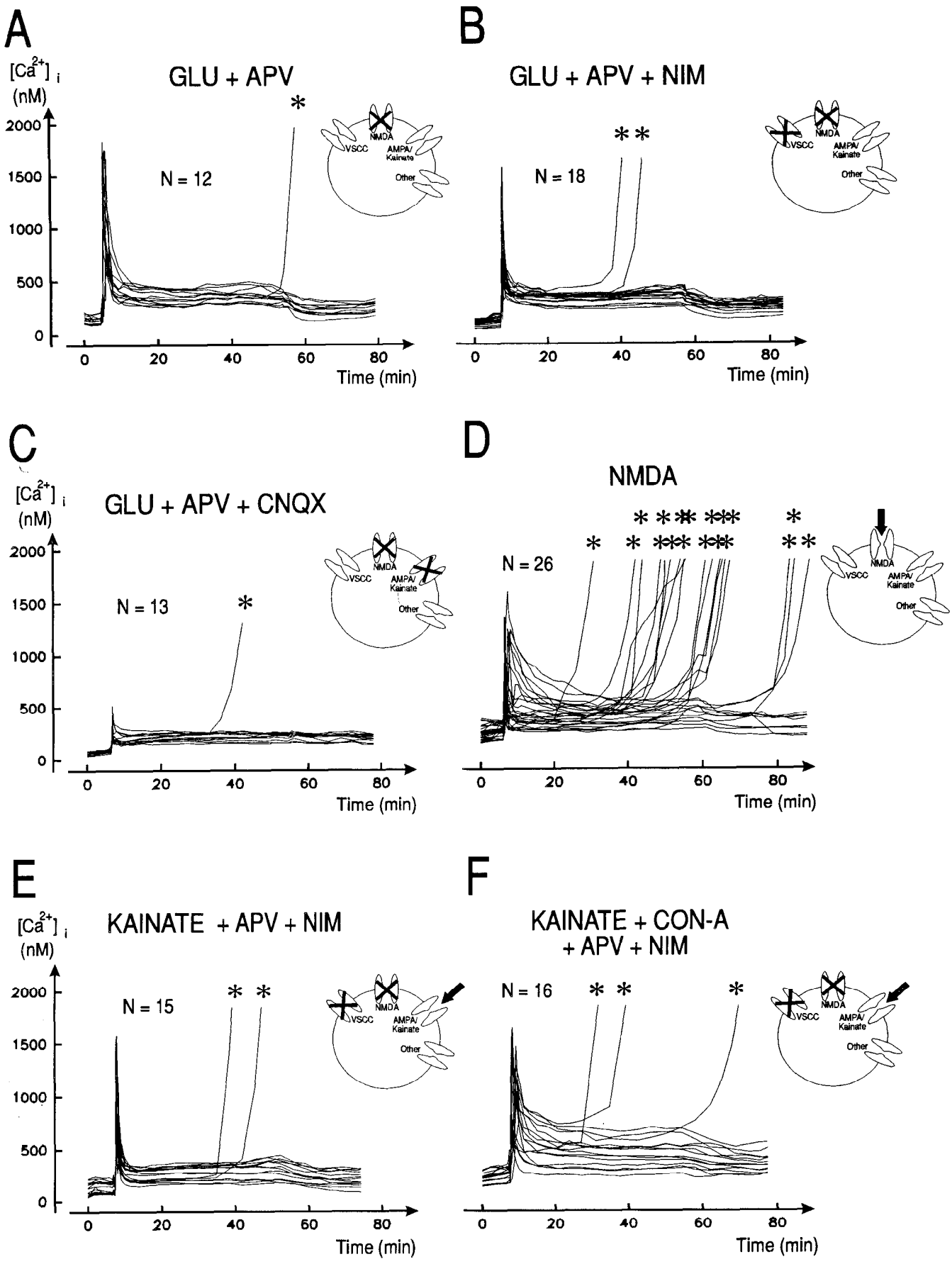
A
GLU + APV
[Ca2+]i (nM)
N = 12
NMDA
VSCC
AMPA/ Kainate
Other
Time (min)
B
GLU + APV + NIM
N = 18
C
GLU + APV + CNQX
N = 13
D
NMDA
N = 26
E
KAINATE + APV + NIM
N = 15
F
KAINATE + CON-A + APV + NIM
N = 16

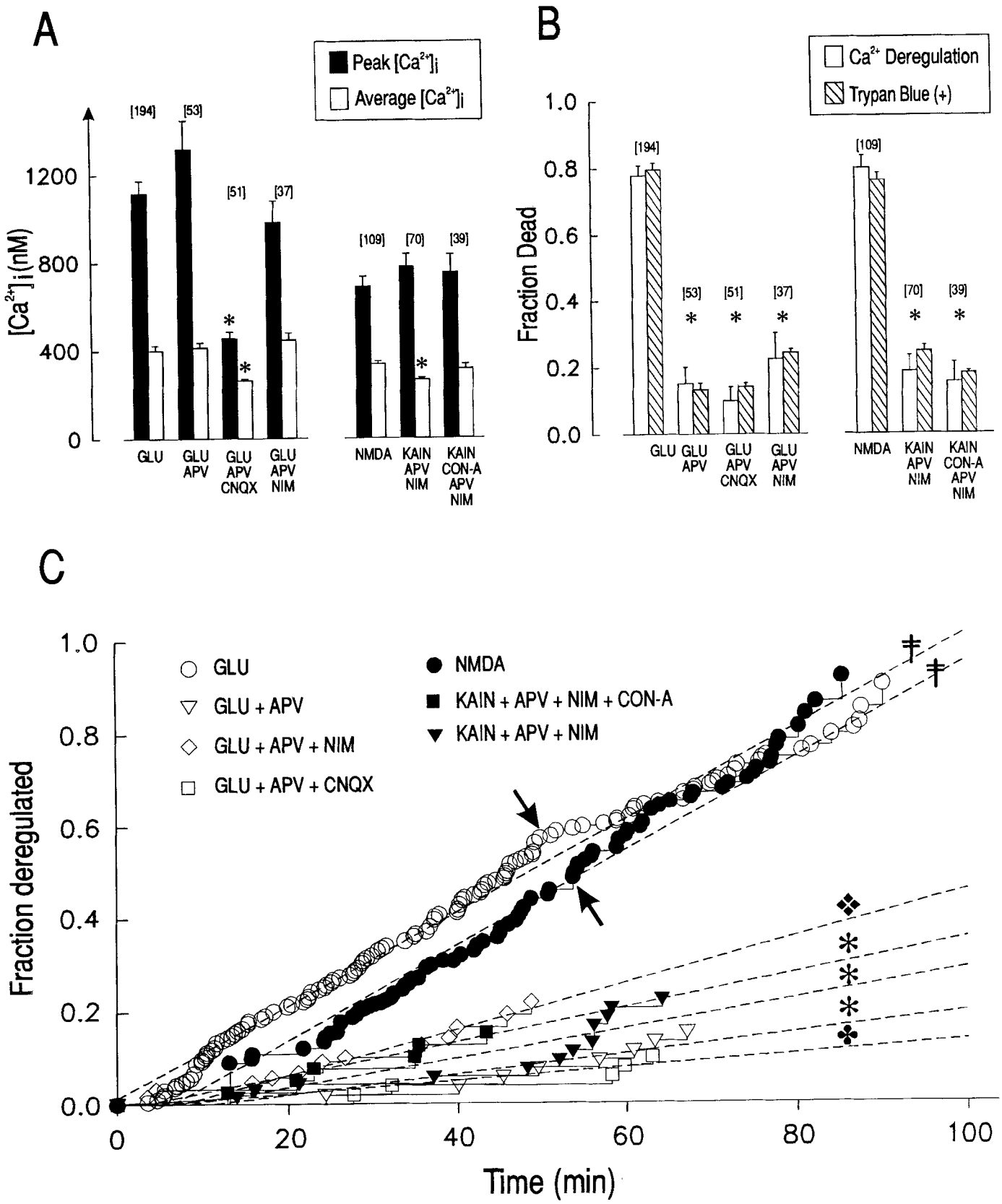

Figure 10. Specificity of glutamate-triggered Ca^{2+} neurotoxicity to the NMDA receptor. A total of 553 neurons were studied using seven combinations of agonists and antagonists of EAA receptors and Ca^{2+} channels as in Figure 9. In *A* and *B*, the numbers of neurons in each group (*in brackets*) were pooled from 5–15 experiments. *Asterisks* denote statistical significance at the $p < 0.0001$ level. *A*, Comparison of peak and average $[Ca^{2+}]_i$ in the seven experimental groups. Note that a 250 μM glutamate challenge evoked similar rises in $[Ca^{2+}]_i$ irrespective of NMDA or Ca^{2+} channel blockade. This rise was effectively attenuated by blocking both NMDA and non-NMDA receptors. *B*, Comparison of neuronal death between groups by Ca^{2+} deregulations (*open bars*) and trypan blue staining (*hatched bars*). Note the excellent agreement between the two methods.

Table 3. Linear and logistic regression modeling of the probability of Ca^{2+} deregulation as a function of Ca^{2+} source, time, peak $[Ca^{2+}]_i$, average $[Ca^{2+}]_i$ and CTI

Parameters	Linear regression	Logistic regression
	$R^2 = 0.638$*	
Source, time, peak, average, CTI	<0.0001, <0.0001, 0.0028, 0.0027, 0.1031	
	$R^2 = 0.637$*	
Source, time, peak, average	<0.0001, <0.0001, 0.0006, 0.0105	
	$R^2 = 0.632$*	LR $\chi^2 = 266.91$, $p = 1.0000$
Source, time, peak	<0.0001, <0.0001, 0.0004	<0.0001, <0.0001, 0.0024
	$R^2 = 0.624$*	LR $\chi^2 = 239.35$, $p = 0.9998$
Source, time	<0.0001, <0.0001	<0.0001, <0.0001
	$R^2 = 0.431$*	LR $\chi^2 = 320.88$, $p = 0.0132$
Time	<0.0001	<0.0001
	$R^2 = 0.377$*	not an ordinal variable
Source	<0.0001	<0.0001

Linear and logistic regressions (left and right data columns, respectively) were employed to model the probability of Ca^{2+} deregulation (P_d) using different combinations of measured experimental parameters derived from experiments on 553 neurons. This approach was used to determine which parameters were important to predicting survival outcome. The linear regression technique employed a least-squares algorithm, whereas the logistic regression technique employed a maximal likelihood estimate approach (see Chaps. 10 and 12 in Armitage and Berry, 1987). It is assumed in these models that the outcome variables (P_d and logit[P_d] for linear and logistic regressions, respectively) are best determined by linear combinations of predictor variables. The predictor variables were source (Ca^{2+} source), time (time to deregulation), peak (Peak $[Ca^{2+}]_i$), average (average $[Ca^{2+}]_i$), and CTI (calcium–time index). Data are the results of a model containing the indicated number of parameters, and contains an index of goodness of fit as well as probabilities of significance of the individual parameters. The goodness of fit of each model to the raw data is indicated by R^2 (multiple correlation coefficient) for linear regression, and by the likelihood ratio (LR) χ^2 for logistic regression, where p is the probability of a perfect fit of the model to the data (0–1.0 indicates zero to perfect fit, respectively). The asterisk indicates that the estimate of R^2 was different from zero at a significance level of <0.0001. In the case of logistic regression analysis, note that LR χ^2 cannot be computed for source alone, as it is not an ordinal variable.

important parameters in creating a predictive relationship between Ca^{2+} and neurotoxicity. These conclusions were consistent with those drawn from our earlier (Fig. 4*D,F,G*; Table 2) and present results: Figure 10*C* shows that when the fraction of deregulated neurons in each experimental group was plotted against time (Kaplan–Meier survival model), there was an almost linear dependence of Ca^{2+} deregulation on time within each group. These data confirm that both Ca^{2+} source and the time dependence of neurotoxicity must be considered in relating $[Ca^{2+}]_i$ to cell death.

We showed that the relationship between $[Ca^{2+}]_i$ and cell death was not evident in a simple correlative analysis involving only two parameters (Fig. 3*B*). However, by taking a more complex statistical approach, we were able to resolve relationships that were not directly obvious, by using models that adjusted for the effects of confounding variables. By this method, when source and time were taken into account by the model, significant relationships between the probability of Ca^{2+} deregulation and peak and average $[Ca^{2+}]_i$ became evident (Table 3). For example, in the linear regression model incorporating source, time, peak, and average, the latter two parameters were significant at $p < 0.0006$ and 0.0105, respectively. However, as shown above, source and time were far greater determinants of neurotoxicity than peak and average $[Ca^{2+}]_i$ because they alone sufficed to predict the probability of Ca^{2+} deregulation.

Discussion

In this article we described the effects of changes in $[Ca^{2+}]_i$ in spinal neurons on neurotoxicity. We showed that when neurons were exposed to a lethal Ca^{2+} challenge, their ability to maintain Ca^{2+} homeostasis failed prior to a loss of plasma membrane integrity (Ca^{2+} deregulation; Fig. 1). Using this and conventional methods for assessing neuronal survival, we showed that in the case of glutamate-triggered neurotoxicity, cell death was dependent on Ca^{2+} influx (Fig. 2*B,C*). Glutamate neurotoxicity was also a function of challenge duration and of submembrane $[Ca^{2+}]_i$, as deduced from the dependence of neuronal death on the transmembrane Ca^{2+} gradient (Fig. 4*A*). Our imaging of $[Ca^{2+}]_i$ showed that there was a "ceiling" on measurable $[Ca^{2+}]_i$ (Fig. 4*B*), a fact that contributed to the difficulty in relating $[Ca^{2+}]_i$ and neurotoxicity using simple linear relationships (Fig. 3*B*). By evoking Ca^{2+} influx into neurons through different pathways (Figs. 5, 6), we demonstrated that neurotoxicity was dependent not only on a large rise in $[Ca^{2+}]_i$, but also on the Ca^{2+} source. Thus, given

←

C, Kaplan–Meier survival plots showing the fraction of Ca^{2+} deregulations as a function of time for each group. These demonstrate that the probability of Ca^{2+} deregulation increases almost linearly with time in all groups, but differs markedly between groups with and without NMDA receptor activation. The slopes of the best-fit straight lines (*broken lines*) reflect the time dependence of Ca^{2+} deregulation. Slopes with the same symbols (*asterisks* or *crosses*) were statistically similar. The mean slope with NMDA blockade was 0.0055, whereas the mean slope without NMDA blockade was twice as steep (0.0134). The median survival times for neurons following NMDA and glutamate exposures were 54.2 min and 46.1 min, respectively (*arrows*).

the same elevations in $[Ca^{2+}]_i$, the neurotoxicity evoked by glutamate far exceeded that evoked by membrane depolarization with high K^+ (Figs. 7, 8). More specifically, the neurotoxicity of glutamate in these experiments was triggered primarily by Ca^{2+} influx through NMDA receptor–gated channels (Fig. 9). NMDA-triggered cell death exceeded that triggered by non-NMDA receptors and Ca^{2+} channels when $[Ca^{2+}]_i$ was made to rise equally through these separate pathways (Fig. 10*A,B*). This confirms that the greater neurotoxicity of NMDA receptors as compared with others is not related to the ability of NMDA channels to trigger greater elevations in $[Ca^{2+}]_i$. In addition, we were able to confirm using statistical modeling that Ca^{2+} source and Ca^{2+} challenge duration were the primary determinant of the likelihood of neuronal survival. Finally, when these two factors were taken into account, a statistically significant relationship between measured $[Ca^{2+}]_i$ and cell death was uncovered (Table 3).

Significance of the Ca^{2+} deregulation phenomenon

Neurons exposed to a lethal Ca^{2+} challenge lost their ability to maintain Ca^{2+} homeostasis. This was manifest as an uncontrolled secondary rise in $[Ca^{2+}]_i$ occurring as early as 30–40 min before plasma membrane integrity was lost (as gauged with trypan blue; Fig. 1). This secondary $[Ca^{2+}]_i$ rise (Ca^{2+} deregulation) inevitably preceded cell death, and was the product of the primary Ca^{2+} insult. This is supported by the finding that Ca^{2+} deregulation was a function of glutamate challenge duration (Figs. 4*D,F,G*; 10*C*; Tables 2, 3) and of transmembrane Ca^{2+} gradient (Fig. 4*A*). Also, it was absolutely dependent on the presence of extracellular Ca^{2+} during the phase that preceded its onset. Its likelihood was substantially reduced by pretreating neurons with APV (Fig. 9*A–C*, 10*B*), but this protective effect diminished greatly when APV was applied more than 30 min following glutamate application (data not shown). This evidence is insufficient to determine whether secondary Ca^{2+} overload caused the ensuing cell death, or whether Ca^{2+} overload occurred prior to—but independently of—the loss of plasma membrane integrity. We favor the latter hypothesis, because as shown by us and others (Randall and Thayer, 1992; M. Tymianski and M. P. Charlton, unpublished observations), neuronal death became independent of $[Ca^{2+}]_i$ once Ca^{2+} deregulation occurred. Nevertheless, the virtual 1:1 relationship between Ca^{2+} deregulation and eventual trypan blue staining makes secondary Ca^{2+} overload a useful early index of impending cell death. The biphasic nature of neurotoxic $[Ca^{2+}]_i$ increases illustrates that the temporal relationships between $[Ca^{2+}]_i$ and neurotoxicity must be considered in order to interpret the relevant $[Ca^{2+}]_i$ measurements appropriately.

Relationship between $[Ca^{2+}]_i$ and neurotoxicity

We and others have shown that simple linear relationships were inadequate to demonstrate a significant relationship between $[Ca^{2+}]_i$ measurements and neuronal death (Fig. 3*B*; Michaels and Rothman, 1990; Dubinsky and Rothman, 1991; Randall and Thayer, 1992). Experimentally, we illustrated that when the Ca^{2+} challenge duration was constant (i.e., 50 min), the critical missing factor in relating $[Ca^{2+}]_i$ to cell death was the Ca^{2+} source (Figs. 7–10). In fitting the data to a number of statistical models (Table 3), we demonstrated that the Ca^{2+} source was considerably more important to predicting the likelihood of cell death than were the actual measured $[Ca^{2+}]_i$ values. Nevertheless, in statistical models that adjusted for the confounding effects of the Ca^{2+} source, we were able to unmask significant relationships between $[Ca^{2+}]_i$ and neurotoxicity. However, we stress that the purpose of our statistical models was to seek descriptive relationships rather than causality. Therefore, the models in themselves do not prove that Ca^{2+} was the cause of neurotoxicity.

Causality between Ca^{2+} influx and neurotoxicity

Was the neurotoxicity of glutamate caused by Ca^{2+}? A simpler alternative is that toxicity was triggered by ions other than Ca^{2+}. This has been examined in this report and detailed in others (Rothman, 1985; Garthwaite et al., 1986; Olney et al., 1986; Rothman and Olney, 1986; Choi, 1987, 1988; Farooqui and Horrocks, 1991). Although glutamate- and particularly NMDA-operated channels are permeable to Na^+ and K^+ in addition to Ca^{2+}, we showed that the former two were unlikely to trigger independently the neurotoxicity observed in the present report, first, because substituting Na^+ for choline (Fig. 2*E*) had little impact on glutamate neurotoxicity; second, because bath application of high K^+ (simulating the changes in transmembrane K^+ gradients following opening of K^+-permeable channels) was not neurotoxic (Figs. 7, 8); third, because extracellular Ca^{2+} was essential to trigger glutamate neurotoxicity (Fig. 2*B,C*); and fourth, because having tested the effects of glutamate in variable concentrations of $[Ca^{2+}]_e$, we showed that neurotoxicity was a function of transmembrane Ca^{2+} gradient rather than of any Ca^{2+}-independent processes (which remained unaltered by virtue of the fixed glutamate challenge; Fig. 4*A*).

The demonstration of the dependence of glutamate neurotoxicity on extracellular Ca^{2+} (Fig. 2*B,C*) has generally been interpreted as a requirement for Ca^{2+} influx (see references in preceding paragraph). An interesting alternative is that extracellular Ca^{2+} could be required for the binding of glutamate to its receptor. This would explain the complete absence of neurotoxicity upon removal of extracellular Ca^{2+}. However, current evidence is contrary to this hypothesis, because the binding of L-glutamate to kainate receptors is actually facilitated by removing extracellular Ca^{2+}, whereas binding to other EAA receptors is not greatly affected by either Ca^{2+} or Cl^- (Dingledine et al., 1988).

Interpretation of the source specificity hypothesis

Our data point to the NMDA receptor channel as the most significant source for neurotoxic Ca^{2+} influx. Although the neurotoxic consequences of NMDA receptor activation are well recognized (Simon et al., 1984; Choi et al., 1987, 1988; Goldberg et al., 1987; Rothman and Olney, 1987; Barnes, 1988; Novelli et al., 1988; Ellren and Lehmann, 1989; Tecoma et al., 1989; Regan and Choi, 1991), we were able to show quantitatively that this toxicity was not due to the ability of NMDA receptors to trigger greater initial $[Ca^{2+}]_i$ increases than other pathways, but rather to some other attribute specifically associated with NMDA-mediated Ca^{2+} influx. We suggest that the rate-limiting processes that trigger early Ca^{2+}-dependent neurotoxicity may be preferentially associated with NMDA receptors. One possibility is that the molecules involved in those processes are physically located in the submembrane region closely surrounding NMDA channels, and are thereby preferentially activated by Ca^{2+} influx through this source. Under this hypothesis, Ca^{2+} influx through alternate sources such as voltage-gated Ca^{2+} channels would be insufficient to trigger cell death because these influx pathways aren't linked with neurotoxic processes. By the time that Ca^{2+} diffuses from these alternate sources, the resultant

$[Ca^{2+}]_i$ in the vicinity of NMDA receptors and their associated trigger sites for Ca^{2+} neurotoxicity would not suffice to cause neurotoxicity (Fig. 11). Our findings may partly explain why certain Ca^{2+} blocking strategies, particularly those employing blockers of voltage-gated Ca^{2+} channels, are unsuccessful in preventing early neurotoxicity *in vitro* and *in vivo* (e.g., Kass et al., 1988; Shi et al., 1989; Madden et al., 1990; Weiss et al., 1990): although these agents successfully lessen Ca^{2+} entry, Ca^{2+} influx through these pathways may not be neurotoxic, and might even have some beneficial effects on long-term neuronal calcium homeostasis and survivability (Gallo et al., 1987; Collins et al., 1991).

Implicit in the assumption that NMDA receptors are preferentially associated with neurotoxic processes is the notion that Ca^{2+}-dependent processes in neurons are compartmentalized along with specific Ca^{2+} influx pathways. There now exists substantial evidence that Ca^{2+} fluxes in neurons are compartmentalized both spatially and temporally. For example, Ca^{2+} channels are strategically distributed throughout the plasma membrane so as to maximize Ca^{2+} influx in subcellular regions subserving relevant cellular functions (Lipscombe et al., 1988; Jones et al., 1989; Robitaille et al., 1990; Westenbroek et al., 1990; Cohen et al., 1991). Similarly, it is suggested that NMDA receptors are clustered throughout neurons on synapses (Jones and Baughman, 1991), dendritic spines (Connor et al., 1988; Muller and Connor, 1991), and neuronal somata (Jones et al., 1990; O. T. Jones, personal communication), thereby optimizing Ca^{2+} fluxes in relevant areas. There is also confirmation that subcellular Ca^{2+} transients can have different temporal profiles in different compartments. For example, intense afferent stimulation can evoke long-lasting $[Ca^{2+}]_i$ gradients between hippocampal dendritic spines and dendritic shafts even in the absence of a physical diffusion barrier (Guthrie et al., 1991; Muller and Connor, 1991).

Concurrently with evidence for compartmentalization of Ca^{2+} fluxes, studies have shown that activation of glutamate receptors, particularly of the NMDA subtype, is associated with initiating a number of secondary processes known to occur in neuronal injury. These include the formation of free radicals (Pellegrini-Giampietro et al., 1990), initiation of the arachidonic acid cascade (Dumuis et al., 1988; Lazarewicz et al., 1990; Sanfeliu et al., 1990), and activation of proteases (Siman et al., 1989), lipases (Farooqui and Horrocks, 1991), and nitric oxide (Beckman, 1991; Dawson et al., 1991; East and Garthwaite, 1991). According to our hypothesis, rate-limiting substrates or enzymes governing these reactions may be found in high concentrations near NMDA-gated channels.

Our experimental paradigms relied on the assumption that $[Ca^{2+}]_i$ could be made to increase to equal levels by activating different Ca^{2+} influx pathways. However, due to limitations on the spatial and temporal resolution of our measurements, we cannot assume that equal $[Ca^{2+}]_i$ transients produced by different agonists reflected equal contributions to $[Ca^{2+}]_i$ by Ca^{2+} influx, Ca^{2+} buffering, and Ca^{2+} release from internal stores. Thus, it is conceivable that different agonists elicit comparable cytosolic $[Ca^{2+}]_i$ increases through different proportional contributions from critical Ca^{2+} compartments. However, this possibility does not detract from our original conclusions. For example, we observed that given equivalent measurable $[Ca^{2+}]_i$ increases, glutamate was more neurotoxic than high K^+. However, it is currently believed that elevations in $[Ca^{2+}]_i$ caused by membrane depolarization (as with high K^+) are almost exclusively mediated by Ca^{2+} influx (Thayer and Miller 1990), whereas measured $[Ca^{2+}]_i$ increases following glutamate application may include a contribution from internally released Ca^{2+} (Murphy and Miller, 1988; Miller, 1992). Thus, given equal increases in total measured $[Ca^{2+}]_i$, glutamate should evoke a lesser contribution to the $[Ca^{2+}]_i$ increase through Ca^{2+} influx. This reasoning lends further credence to the source specificity hypothesis, because it suggests that lesser Ca^{2+} fluxes through glutamate-gated channels trigger more neurotoxicity than greater Ca^{2+} fluxes through voltage-gated Ca^{2+} channels.

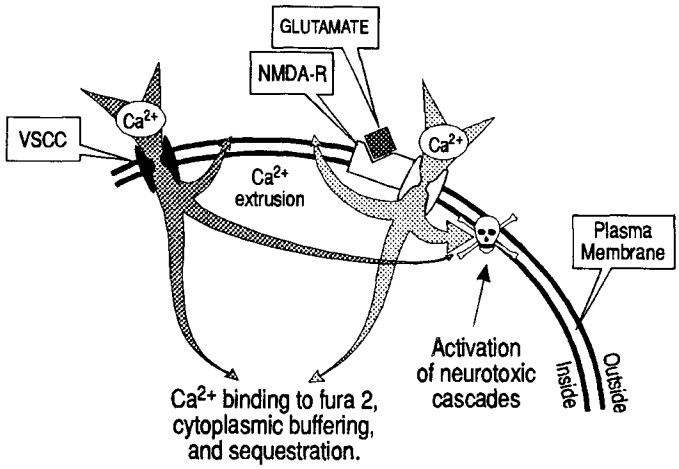

Figure 11. Schematic of the source specificity hypothesis relating Ca^{2+} influx, Ca^{2+} source, Ca^{2+}-triggered neurotoxicity, and measured cytoplasmic $[Ca^{2+}]_i$. Neurotoxicity is assumed to be triggered in physical proximity to NMDA channels. Therefore, Ca^{2+} that diffuses from non-NMDA channels reaches the vicinity of NMDA receptors at insufficient concentrations to trigger neurotoxicity. *VSCC*, voltage-gated Ca^{2+} channel; *NMDA-R*, NMDA receptor channel complex. The *arrows* represent the magnitude of Ca^{2+} fluxes generated by VSCCs and NMDA-R.

A theoretical corollary to the above is that $[Ca^{2+}]_i$ transients could be buffered with different efficiencies when they are triggered by different pathways. Under this assumption, when equal $[Ca^{2+}]_i$ transients are measured following high K^+ and glutamate challenges, $[Ca^{2+}]_i$ in the critical submembrane shell might be unequal due to less efficient buffering of one Ca^{2+} source as compared with the other. This hypothesis explains Ca^{2+} neurotoxicity in terms of the ability of a given Ca^{2+} influx pathway to raise submembrane $[Ca^{2+}]_i$. This alternative to the source specificity hypothesis (Fig. 11) requires that cytoplasmic Ca^{2+} buffers be preferentially compartmentalized with a given class of Ca^{2+} sources, rather than requiring that these sources be colocalized with Ca^{2+} neurotoxicity "trigger sites." A second theoretical possibility is that elevated $[Ca^{2+}]_i$ triggers neurotoxicity by acting synergistically with some undiscovered (glutamate-triggered, Ca^{2+}-independent) process associated specifically with NMDA receptors. Under this possibility, neurotoxic Ca^{2+} elevations may be produced by mechanisms not involving influx specifically through NMDA receptor channels as long as $[Ca^{2+}]_i$ still reaches "toxic" levels in the vicinity of NMDA receptors.

The timing of NMDA neurotoxicity

Our experiments do not preclude the possibility that EAA toxicity in spinal neurons can occur both through NMDA and non-NMDA glutamate receptor activation. Previous observations in cultured cortical and hippocampal neurons (Rothman et al.,

1987; Koh and Choi, 1991) showed that selective blockade of non-NMDA receptors did not block early neuronal death triggered by brief (<20 min) glutamate exposure at room temperature, whereas both NMDA and non-NMDA agonists could evoke delayed neurotoxicity (occurring several hours after agonist application). The observed preponderance of NMDA neurotoxicity in the present study may have been influenced by the short duration of our observation period, the relatively long duration of the agonist challenge (50 min), and the fact that all agonist exposures were performed at 36.5°C rather than at room temperature. Our results showed that given equivalent Ca^{2+} loads, NMDA triggered neurotoxicity more rapidly than non-NMDA glutamate receptor agonists (Fig. 10*C*). However, the timing and extent of maximal non-NMDA neurotoxicity in our experimental model remain subjects for future investigation.

Summary

This report shows that early EAA-mediated neurotoxicity is dependent on the influx of Ca^{2+} ions into neurons, and is heralded by a failure to maintain Ca^{2+} homeostasis. The likelihood of Ca^{2+} homeostatic failure and cell death is a function of transmembrane Ca^{2+} flux, which is inadequately reflected by conventional $[Ca^{2+}]_i$ measurements. The chief predictors of neuronal death are the source of Ca^{2+} influx and the duration of agonist application. These must be taken into account in relating $[Ca^{2+}]_i$ to neuronal survival outcome. In the case of the most neurotoxic Ca^{2+} source, the NMDA receptor channel, neurotoxicity was not caused by its ability to cause greater measured $[Ca^{2+}]_i$ increases than other Ca^{2+} sources, but rather by some attribute specific to the NMDA receptor channel complex. We hypothesize that this attribute consists of the physical colocalization of NMDA receptors with Ca^{2+}-dependent rate-limiting processes that trigger neuronal degeneration.

References

Armitage P, Berry G (1987) Statistical methods in medical research. Oxford: Blackwell.

Artalejo CR, Perlman RL, Fox AP (1992) ω-Conotoxin GVIA blocks a Ca^{2+} current in bovine chromaffin cells that is not of the "classic" N type. Neuron 8:85–95.

Balentine JD (1988) Spinal cord trauma: in search of the meaning of granular axoplasm and vesicular myelin. J Neuropathol Exp Neurol 47:77–92.

Barnes DM (1988) NMDA receptors trigger excitement [news]. Science 239:254–256.

Beckman JS (1991) The double-edged role of nitric oxide in brain function and superoxide-mediated injury. J Dev Physiol 15:53–59.

Choi DW (1985) Glutamate neurotoxicity in cortical cell culture is calcium dependent. Neurosci Lett 58:293–297.

Choi DW (1987) Ionic dependence of glutamate neurotoxicity. J Neurosci 7:369–379.

Choi DW (1988) Calcium-mediated neurotoxicity: relationship to specific channel types and role in ischemic damage. Trends Neurosci 11: 465–467.

Choi DW, Maulucci-Gedde M, Kriegstein AR (1987) Glutamate neurotoxicity in cortical cell culture. J Neurosci 7:357–368.

Choi DW, Koh JY, Peters S (1988) Pharmacology of glutamate neurotoxicity in cortical cell culture: attenuation by NMDA antagonists. J Neurosci 8:185–196.

Cohen MW, Jones OT, Angelides KJ (1991) Distribution of Ca^{2+} channels on frog motor nerve terminals revealed by fluorescent ω-conotoxin. J Neurosci 11:1032–1039.

Collins F, Schmidt MF, Guthrie PB, Kater SB (1991) Sustained increase in intracellular calcium promotes neuronal survival. J Neurosci 11:2582–2587.

Connor JA, Tseng HY, Hockberger PE (1987) Depolarization- and transmitter-induced changes in intracellular Ca^{2+} of rat cerebellar granule cells in explant cultures. J Neurosci 7:1384–1400.

Connor JA, Wadman WJ, Hockberger PE, Wong RKS (1988) Sustained dendritic gradients of calcium induced by excitatory amino acids in CA1 hippocampal neurons. Science 240:649–653.

Dawson VL, Dawson TM, London ED, Bredt DS, Snyder SH (1991) Nitric oxide mediates glutamate neurotoxicity in primary cortical cultures. Proc Natl Acad Sci USA 88:6368–6371.

Dingledine R, Boland LM, Chamberlin NL, Kawasaki K, Kleckner NW, Traynelis SF, Verdoorn TA (1988) Amino acid receptors and uptake systems in the mammalian central nervous system. CRC Crit Rev Neurobiol 4:1–97.

Dubinsky JM, Rothman SM (1991) Intracellular calcium concentration during "chemical hypoxia" and excitotoxic neuronal injury. J Neurosci 11:2545–2551.

Dumuis A, Sebben M, Haynes L, Pin JP, Bockaert J (1988) NMDA receptors activate the arachidonic acid cascade system in striatal neurons. Nature 336:68–70.

East SJ, Garthwaite J (1991) NMDA receptor activation in rat hippocampus induces cyclic GMP formation through the L-arginine–nitric oxide pathway. Neurosci Lett 123:17–19.

Ellren K, Lehmann A (1989) Calcium dependency of *N*-methyl-D-aspartate toxicity in slices from the immature rat hippocampus. Neuroscience 32:371–379.

Faden AI, Demediuk P, Panter SS, Vink P (1989) The role of excitatory amino acids and NMDA receptors in traumatic brain injury. Science 244:798–800.

Farooqui AA, Horrocks LA (1991) Excitatory amino acid receptors, neural membrane phospholipid metabolism and neurological disorders. Brain Res Rev 16:171–191.

Frandsen A, Schousboe A (1991) Dantrolene prevents glutamate cytotoxicity and Ca^{2+} release from intracellular stores in cultured cerebral cortical neurons. J Neurochem 56:1075–1078.

Gahwiler BH (1981) Organotypic monolayer cultures of nervous tissue. J Neurosci Methods 4:329–342.

Gallo V, Kingsbury A, Balazs R, Jorgensen OS (1987) The role of depolarization in the survival and differentiation of cerebellar granule cells in culture. J Neurosci 7:2203–2213.

Garthwaite G, Hajos F, Garthwaite J (1986) Ionic requirements for neurotoxic effects of excitatory amino acid analogues in rat cerebellar slices. Neuroscience 18:437–447.

Garthwaite J, Garthwaite G (1983) The mechanism of kainic acid neurotoxicity. Nature 305:138–140.

Glaum SR, Scholz WK, Miller RJ (1990) Acute- and long-term glutamate-mediated regulation of $[Ca^{2+}]_i$ in rat hippocampal pyramidal neurons *in vitro*. J Pharmacol Exp Ther 253:1293–1302.

Goldberg MP, Weiss JH, Pham PC, Choi DW (1987) *N*-methyl-D-aspartate receptors mediate hypoxic neuronal injury in cortical culture. J Pharmacol Exp Ther 243:784–791.

Goldberg MP, Giffard RG, Kurth MC, Choi DW (1989) Role of extracellular calcium and magnesium in ischemic neuronal injury *in vitro*. Neurology [Suppl] 39:217.

Goldberg WJ, Kadingo RM, Barrett JN (1986) Effects of ischemia-like conditions on cultured neurons: protection by low Na^+, low Ca^{2+} solutions. J Neurosci 6:3144–3151.

Goldman WF, Bova S, Blaustein MP (1990) Measurement of intracellular Ca^{2+} in cultured arterial smooth muscle cells using fura-2 and digital imaging microscopy. Cell Calcium 11:221–231.

Grynkiewicz G, Poenie M, Tsien RY (1985) A new generation of calcium indicators with greatly improved fluorescence properties. J Biol Chem 260:3440–3450.

Guthrie PB, Brenneman DE, Neale EA (1987) Morphological and biochemical differences expressed in separate dissociated cell cultures of dorsal and ventral halves of the mouse spinal cord. Brain Res 420: 313–323.

Guthrie PB, Segal M, Kater SB (1991) Independent regulation of calcium revealed by imaging dendritic spines. Nature 354:76–80.

Hernandez-Cruz A, Sala F, Adams PR (1990) Subcellular calcium transients visualized by confocal microscopy in a voltage-clamped vertebrate neuron. Science 247:858–862.

Hille B (1992) Ionic channels of excitable membranes, Chaps 13, 14. Sunderland, MA: Sinauer.

Holopainen I, Enkvist MOK, Akerman KEO (1989) Glutamate receptor antagonists increase intracellular calcium independently of voltage-gated calcium channels in rat cerebellar granule cells. Neurosci Lett 98:57–62.

Honore T, Davies SN, Drejer J, Fletcher EJ, Jacobsen P, Lodge D, Nielsen FE (1988) Quinoxalinediones: potent competitive non-NMDA glutamate receptor antagonists. Science 241:701–703.

Jancso G, Karcsu S, Kiraly E, Szebeni A, Toth L, Bacsy E, Joo F, Parducz A (1984) Neurotoxin induced nerve cell degeneration: possible involvement of calcium. Brain Res 295:211–216.

Jones KA, Baughman RW (1991) Both NMDA and non-NMDA subtypes of glutamate receptors are concentrated at synapses on cerebral cortical neurons in culture. Neuron 7:593–603.

Jones OT, Kunze DL, Angelides KJ (1989) Localization and mobility of ω-conotoxin-sensitive Ca^{2+} channels in hippocampal CA1 neurons. Science 244:1189–1193.

Jones OT, McGurk JF, Bennett MVL, Zuckin RS, Collinridge G, Benke T, Angelides KJ (1990) Distribution of NMDA receptors on hippocampal neurons. Soc Neurosci Abstr 16:396.3.

Kass IS, Cottrell JE, Chambers G (1988) Magnesium and cobalt, not nimodipine, protect neurons against anoxic damage in the rat hippocampal slice. Anaesthesiology 69:710–715.

Kauppinen RA, Sihra TS, Nicholls DG (1986) Divalent cation modulation of the ionic permeability of the synaptosomal plasma membrane. Biochim Biophys Acta 860:178–184.

Koh JY, Choi DW (1991) Selective blockade of non-NMDA receptors does not block rapidly triggered glutamate-induced neuronal death. Brain Res 548:318–321.

Koh JY, Goldberg MP, Hartley DM, Choi DW (1990) Non-NMDA receptor-mediated neurotoxicity in cortical culture. J Neurosci 10: 696–705.

Kurth MC, Weiss JH, Choi DW (1989) Relationship between glutamate-induced 45-calcium influx and resultant neuronal injury in cultured cortical neurons. Neurology [Suppl] 39:217.

Lazarewicz JW, Wroblewski JT, Costa E (1990) *N*-methyl-D-aspartate-sensitive glutamate receptors induce calcium-mediated arachidonic acid release in primary cultures of cerebellar granule cells. J Neurochem 55:1875–1881.

Lemasters JJ, DiGiuseppi JD, Nieminen AL, Herman B (1987) Blebbing, free calcium and mitochondrial membrane potential preceding cell death in hepatocytes. Nature 325:78–81.

Lipscombe D, Madison D, Poenie M, Reuter H, Tsien RY, Tsien RW (1988) Spatial distribution of calcium channels and cytosolic transients in growth cones and cell bodies of sympathetic neurons. Proc Natl Acad Sci USA 85:2398–2402.

Madden KP, Clark WM, Marcoux FW, Probert AW Jr, Weber ML, Rivier J, Zivin JA (1990) Treatment with conotoxin, an 'N-type' calcium channel blocker, in neuronal hypoxic-ischemic injury. Brain Res 537:256–262.

Marcoux FW, Probert AW, Weber ML (1990) Hypoxic neuronal injury in tissue culture is associated with delayed calcium accumulation. Stroke [Suppl] 21:III-71—III-74.

Marquardt DW (1963) An algorithm for least-squares estimation of nonlinear parameters. J Soc Ind Appl Math 11:431–441.

Mayer ML, Vyklicky L (1989) Concanavalin A selectively reduces desensitization of mammalian neuronal quisqualate receptors. Proc Natl Acad Sci USA 86:1411–1415.

Mayer ML, MacDermott AB, Westbrook GL, Smith SJ, Barker JL (1987) Agonist- and voltage-gated calcium entry in cultured mouse spinal neurons under voltage clamp measured using arsenazo III. J Neurosci 7:3230–3244.

Meyer FB (1989) Calcium, neuronal hyperexcitability and ischemic injury. Brain Res Rev 14:227–243.

Michaels RL, Rothman SM (1990) Glutamate neurotoxicity *in vitro*: antagonist pharmacology and intracellular calcium concentrations. J Neurosci 10:283–292.

Milani D, Guidolin D, Facci L, Pozzan T, Buso M, Leon A, Skaper SD (1991) Excitatory amino acid-induced alterations of cytoplasmic free Ca^{2+} in individual cerebellar granule neurons: role in neurotoxicity. J Neurosci Res 28:434–441.

Miller RJ (1992) Neuronal Ca^{2+}: getting it up and keeping it up. Trends Neurosci 15:317–319.

Moore EDW, Becker PL, Fogarty KE, Williams DA, Fay FS (1990) Ca^{2+} imaging in single living cells: theoretical and practical issues. Cell Calcium 11:157–179.

Moore PL, MacCoubrey IC, Haugland RP (1990) A rapid, pH insensitive, two color fluorescence viability (cytotoxicity) assay. J Cell Biol 111:58a.

Mosinger JL, Price MT, Bai HY, Xiao H, Wozniak DF, Olney JW (1991) Blockade of both NMDA and non-NMDA receptors is required for optimal protection against ischemic neuronal degeneration in the *in vivo* adult mammalian retina. Exp Neurol 113:10–17.

Muller W, Connor JA (1991) Dendritic spines as individual neuronal compartments for synaptic Ca^{2+} responses. Nature 354:73–80.

Murphy SN, Miller RJ (1988) A glutamate receptor regulates Ca^{2+} mobilization in hippocampal neurons. Proc Natl Acad Sci USA 85: 8737–8741.

Murphy SN, Thayer SA, Miller RJ (1987) The effects of excitatory amino acids on intracellular calcium in single mouse striatal neurons *in vitro*. J Neurosci 7:4145–4158.

Murphy TH, Malouf AT, Sastre A, Schnaar RL, Coyle JT (1988) Calcium-dependent glutamate cytotoxicity in a neuronal cell line. Brain Res 444:325–332.

Novelli A, Reilly JA, Lysko PG, Henneberry RC (1988) Glutamate becomes neurotoxic via the *N*-methyl-D-aspartate receptor when intracellular energy levels are reduced. Brain Res 451:205–212.

Olney JW, Price MT, Samson L, Labruyere J (1986) The role of specific ions in glutamate neurotoxicity. Neurosci Lett 65:65–71.

Opitz T, Reymann KG (1991) Blockade of metabotropic glutamate receptors protects rat CA1 neurons from hypoxic injury. Neuroreport 2:455–457.

Pellegrini-Giampietro DE, Cherici G, Alesiani M, Carla V, Moroni F (1990) Excitatory amino acid release and free radical formation may cooperate in the genesis of ischemia-induced neuronal damage. J Neurosci 10:1035–1041.

Price MT, Olney JW, Samson L, Labruyere J (1985) Calcium influx accompanies but does not cause excitotoxin-induced neuronal necrosis in retina. Brain Res Bull 14:369–376.

Randall RD, Thayer SA (1992) Glutamate-induced calcium transient triggers delayed calcium overload and neurotoxicity in rat hippocampal neurons. J Neurosci 12:1882–1895.

Regan LJ, Sah DWY, Bean BP (1991) Ca^{2+} channels in rat central and peripheral neurons: high-threshold current resistant to dihydropyridine blockers and ω-conotoxin. Neuron 6:269–280.

Regan RF, Choi DW (1991) Glutamate neurotoxicity in spinal cord cell culture. Neuroscience 43:585–591.

Robitaille R, Adler EM, Charlton MP (1990) Strategic location of calcium channels at transmitter release sites of frog neuromuscular synapses. Neuron 5:773–779.

Roe MW, Lemasters JJ, Herman B (1990) Assessment of fura-2 for measurements of cytosolic free calcium. Cell Calcium 11:63–73.

Rosario LM, Soria B, Feuerstein G, Pollard HB (1989) Voltage-sensitive calcium flux into bovine chromaffin cells occurs through dihydropyridine-sensitive and dihydropyridine-insensitive pathways. Neuroscience 29:735–747.

Rothman SM (1984) Synaptic release of excitatory amino acid neurotransmitter mediates anoxic neuronal death. J Neurosci 4:1884–1891.

Rothman SM (1985) The neurotoxicity of excitatory amino acids is produced by passive chloride influx. J Neurosci 5:1483–1489.

Rothman SM, Olney JW (1986) Glutamate and the pathophysiology of hypoxic-ischemic brain damage. Ann Neurol 19:105–111.

Rothman SM, Olney JW (1987) Excitotoxicity and the NMDA receptor. Trends Neurosci 10:299–302.

Rothman SM, Thurston JH, Hauart RE (1987) Delayed neurotoxicity of excitatory amino acids *in vitro*. Neuroscience 22:471–480.

Sanfeliu C, Hunt A, Patel AJ (1990) Exposure to *N*-methyl-D-aspartate increases release of arachidonic acid in primary cultures of rat hippocampal neurons and not in astrocytes. Brain Res 526:241–248.

Schanne FAX, Kane AB, Young EA, Farber JL (1979) Calcium dependence of toxic cell death: a final common pathway. Science 206: 700–702.

Scharfman HE, Schwartzkroin PA (1989) Protection of dentate hilar cells from prolonged stimulation by intracellular calcium chelation. Science 246:257–260.

Scroggs RS, Fox AP (1991) Distribution of dihydropyridine and ω-conotoxin-sensitive calcium currents in acutely isolated rat and frog sensory neuron somata: diameter-dependent L-channel expression in frog. J Neurosci 11:1334–1346.

Shi RY, Lucas JH, Wolf A, Gross GW (1989) Calcium antagonists fail to protect mammalian spinal neurons after physical injury. J Neurotrauma 6:261–278.

Siesjo BK (1988) Mechanisms of ischemic brain damage. Crit Care Med 16:954–963.

Siesjo BK, Bengtsson F (1989) Calcium fluxes, calcium antagonists, and calcium-related pathology in brain ischemia, hypoglycemia, and

spreading depression: a unifying hypothesis. J Cereb Blood Flow Metab 9:127–140.

Siman R, Noszek C, Kegerise C (1989) Calpain I activation is specifically related to excitatory amino acid induction of hippocampal damage. J Neurosci 9:1579–1590.

Simon RP, Swan JH, Meldrum BS (1984) Blockade of *N*-methyl-D-aspartate receptors may protect against ischemic damage in the brain. Science 226:850–852.

Swandulla D, Hans M, Zipser K, Augustine GJ (1991) Role of residual calcium in synaptic depression and posttetanic potentiation: fast and slow calcium signaling in nerve terminals. Neuron 7:915–926.

Tecoma ES, Monyer H, Goldberg MP, Choi DW (1989) Traumatic neuronal injury *in vitro* is attenuated by NMDA antagonists. Neuron 2:1541–1545.

Thayer SA, Miller RJ (1990) Regulation of the intracellular free calcium concentration in single rat dorsal root ganglion neurones in vitro. J Physiol (Lond) 425:85–115.

Uematsu D, Araki N, Greenberg JH, Reivitch M (1990) Alterations in cytosolic free calcium in the cat cortex during bicuculline-induced epilepsy. Brain Res Bull 24:285–288.

Uematsu D, Araki N, Greenberg JH, Sladky J, Reivich M (1991) Combined therapy with MK-801 and nimodipine for protection of ischemic brain damage [see comments]. Neurology 41:88–94.

Urca G, Urca R (1990) Neurotoxic effects of excitatory amino acids in the mouse spinal cord: quisqualate and kainate but not *N*-methyl-D-aspartate induce permanent neural damage. Brain Res 529:7–15.

Watkins JC, Krogsgaard-Larsen P, Honore T (1990) Structure-activity relationships in the development of excitatory amino acid receptor agonists and competitive antagonists. Trends Pharmacol Sci 11:25–33.

Weiss JH, Hartley DM, Koh J, Choi DW (1990) The calcium channel blocker nifedipine attenuates slow excitatory amino acid neurotoxicity. Science 247:1474–1477.

Westenbroek RE, Ahlijanian MK, Catterall WA (1990) Clustering of L-type Ca^{2+} channels at the base of major dendrites in hippocampal neurons. Nature 347:281–284.

Williams DA, Fay FS (1990) Intracellular calibration of the fluorescent calcium indicator fura-2. Cell Calcium 11:75–83.

Yuste R, Katz LC (1991) Control of postsynaptic Ca^{2+} influx in developing neocortex by excitatory and inhibitory neurotransmitters. Neuron 6:333–344.

Zorumski CF, Thio LL (1992) Properties of vertebrate glutamate receptors: calcium mobilization and desensitization. Prog Neurobiol 39:295–336.